

An ansatz to the quantum phase transition in a dissipative two-qubit system

Hang Zheng¹, Zhiguo Lü¹, and Yang Zhao²

¹Key Laboratory of Artificial Structures and Quantum Control (Ministry of Education), Department of Physics, Shanghai Jiao Tong University, Shanghai 200240, China

²Division of Materials Science, Nanyang Technological University, Singapore 639798, Singapore

Abstract

By means of a unitary transformation, we propose an ansatz to study quantum phase transitions in the ground state of a two-qubit system interacting with a dissipative reservoir. First, the ground state phase diagram is analyzed in the presence of the Ohmic and sub-Ohmic bath using an analytic ground state wave function which takes into account the competition between intrasite tunneling and intersite correlation. The quantum critical point is determined as the transition point from non-degenerate to degenerate ground state and our calculated critical coupling strength α_c agrees with that from the numerical renormalization group method. Moreover, by computing the entanglement entropy between the qubits and the bath as well as the qubit-qubit correlation function in the ground state, we explore the nature of the quantum phase transition between the delocalized and localized states.

PACS numbers: 05.30.Rt, 03.65.Yz, 03.75.Ggb

I Introduction

Quantum phase transitions (QPT) in impurity models with competing interactions have been a subject of great interest in recent years. In this work we consider a two-qubit system coupled with a dissipative bath, in which the competing interactions are the intrasite tunneling, the qubit-bath coupling, and the intersite qubit-qubit interaction. The Hamiltonian for the interacting system and environment reads[1]

$$H = \sum_{i=1,2} \left\{ -\frac{\Delta}{2} \sigma_i^x - \frac{\epsilon}{2} \sigma_i^z + \sum_k \frac{g_k}{2} (b_k^\dagger + b_k) \sigma_i^z \right\} + K \sigma_1^z \sigma_2^z + \sum_k \omega_k b_k^\dagger b_k. \quad (1)$$

where b_k^\dagger (b_k) is the creation (annihilation) operator of boson mode with frequency ω_k and σ^x and σ^z are the Pauli matrices where the subscripts denote qubit 1 and 2. Δ is the intrasite tunneling, ϵ is the bias on every qubit, and K is the Ising-type qubit-qubit interaction. Throughout this paper we set $\hbar = 1$. The qubit-bath coupling is denoted by g_k , and the effect of the bath is characterized by a spectral density $J(\omega) = \sum_k g_k^2 \delta(\omega - \omega_k) = 2\alpha\omega^s \omega_c^{1-s} \theta(\omega_c - \omega)$ with the dimensionless coupling strength α and the hard upper cutoff at ω_c . The index s accounts for various physical situations[2, 3]: the Ohmic $s = 1$, sub-Ohmic $s < 1$ and super-Ohmic $s > 1$ baths. In this paper we use a very small bias $\epsilon/\omega_c \leq 10^{-5}$ to trigger the QPT[1].

The QPT is a ground state transition when the parameter of Hamiltonian changes across some critical point. If the qubits and bath are decoupled, $g_k = 0$, Hamiltonian (1) can be solved easily and there is no QPT if we keep a very small bias $\epsilon/\omega_c \leq 10^{-5}$. The QPT is triggered by competing interactions: The intrasite tunneling Δ favors the delocalized state with $\langle \sigma_i^z \rangle_G \approx 0$, where $i = 1, 2$ and $\langle \dots \rangle_G$ denotes the ground state average. But the role of a finite qubit-bath coupling strength ($g_k \neq 0$, or finite α) is to ensure dissipation in the qubits[2, 3], which competes with the tunneling effect and leads to the possibility of localization with a finite value of $\langle \sigma_i^z \rangle_G$. The QPT in the single-qubit spin-boson model (SBM) was studied by many authors and its properties are well-understood. Various numerical methods were used for this purpose, such as the numerical renormalization group (NRG)[4, 5, 6], the quantum Monte Carlo (QMC)[7], the method of sparse polynomial space representation[8], the extended coherent state

approach[9], and the variational matrix product state approach[10]. In addition, an extension of the Silbey-Harris [11] ground state has been recently employed by us [12] to study the QPT of the single-qubit SBM in the Ohmic ($s = 1$) and sub-Ohmic ($s < 1$) bath.

For the two-qubit SBM described by Eq. (1) where the qubits interact with a common bath, the QPT may differ significantly from that of the single-qubit SBM because the qubit-bath interaction may induce an effective Ising-type ferromagnetic coupling between qubits which is superposed on the original Ising coupling K and leads to a renormalized Ising coupling $(K - V)\sigma_1^z\sigma_2^z$, where $-V$ is the induced coupling strength [1]. For the two-qubit SBM with the Ohmic bath ($s = 1$), McCutcheon *et al.* predicted variationally the quantum critical point (QCP) at $\alpha_c = 0.5$ in the absence of both bias ($\epsilon = 0$) and direct Ising couple ($K = 0$) [13]. Using the numerical renormalization group, however, Orth *et al.*[1] arrived at $\alpha_c \approx 0.15$. Recently, Winter and Rieger studied the quantum phase transition of multi-qubit SBM for $K = 0$ with the help of extensive quantum Monte Carlo simulations[14]. They found $\alpha_c \approx 0.2$ for $\Delta/\omega_c = 0.1$ in the Ohmic bath.

In this work we present a new analytical approach based on a unitary transformation. We will show that due to the renormalized Ising coupling the QCP of the two-qubit SBM acquires a substantial shift as compared to that of the single-qubit case. In addition, the qubit-bath entanglement entropy will be calculated to see how the parameters in (1), Δ , α , and K , compete with each other and lead to the delocalization-localization transition.

The remainder of the paper is organized as follows. In Section II, the unitary transformation of the Hamiltonian is introduced, and the ground state properties are discussed. Implications of our results to the quantum phase transition are elaborated in Section III. The entanglement entropy between the qubits and the bath and the qubit-qubit correlation function are studied in sections IV and V, respectively. Finally, conclusions are drawn in Section VI.

II Unitary transformation

In order to find the ground state, we apply a unitary transformation on Hamiltonian (1), i.e., $H' = \exp(S)H \exp(-S)$, with the generator S given by

$$S = \sum_{\mathbf{k}} \frac{g_{\mathbf{k}}}{2\omega_{\mathbf{k}}} (b_{\mathbf{k}}^{\dagger} - b_{\mathbf{k}}) [\xi_{\mathbf{k}}(\sigma_1^z + \sigma_2^z) + (1 - \xi_{\mathbf{k}})\sigma_0]. \quad (2)$$

where σ_0 is a number and ξ_k is a function of ω_k . Compared with the ground state of Ref.[13], a finite number σ_0 is introduced to take into account the modified bias $\epsilon \rightarrow \epsilon'$ (when $\epsilon \neq 0$) because of the qubit-bath interaction[15, 16, 17]. The form of σ_0 and ξ_k will be determined later. After the transformation, we obtain

$$H' = H'_0 + U_{\epsilon} + H'_1 + H'_2, \quad (3)$$

$$H'_0 = -\eta\Delta(\sigma_1^x + \sigma_2^x)/2 + (K - V)\sigma_1^z\sigma_2^z + \sum_k \omega_k b_k^{\dagger} b_k - V + F\sigma_0^2/4, \quad (4)$$

$$U_{\epsilon} = -\epsilon'(\sigma_1^z + \sigma_2^z)/2, \quad \epsilon' = \epsilon + F\sigma_0 \quad (5)$$

$$H'_1 = \sum_k g_k (b_k^{\dagger} + b_k)(1 - \xi_k)(\sigma_1^z + \sigma_2^z - \sigma_0)/2 - \eta\Delta \sum_k \frac{g_k}{2\omega_k} \xi_k (b_k^{\dagger} - b_k)(i\sigma_1^y + i\sigma_2^y), \quad (6)$$

$$H'_2 = -\frac{\Delta}{2}(\sigma_1^x + \sigma_2^x) \{\cosh(Y) - \eta\} - \frac{\Delta}{2}(i\sigma_1^y + i\sigma_2^y) \{\sinh(Y) - \eta Y\}, \quad (7)$$

where $F = \sum_k g_k^2(1 - \xi_k)^2/\omega_k$ and $Y = \sum_k g_k \xi_k (b_k^{\dagger} - b_k)/\omega_k$. In the zeroth-order transformed Hamiltonian H'_0 ,

$$\eta = \exp \left\{ - \sum_k \frac{g_k^2}{2\omega_k^2} \xi_k^2 \right\} \quad (8)$$

is the environment dressing of the bare tunneling Δ , and

$$V = \sum_k \frac{g_k^2}{2\omega_k} \xi_k (2 - \xi_k) \quad (9)$$

is the bath induced Ising-type interaction. Note that in H'_0 the Ising-type interaction is modified by the qubit-bath coupling: $K' = K - V$. Besides, ϵ' in Eq.(5) is the modified bias which is related to the number σ_0 introduced in our transformation.

With only the Ising-type interaction, the zeroth-order Hamiltonian H'_0 may be diagonalized by the following two-qubit states,

$$|A\rangle = [(u+v)|11\rangle + (u-v)|22\rangle] / \sqrt{2}, \quad (10)$$

$$|B\rangle = [|12\rangle + |21\rangle] / \sqrt{2}, \quad (11)$$

$$|C\rangle = [|12\rangle - |21\rangle] / \sqrt{2}, \quad (12)$$

$$|D\rangle = [(v-u)|11\rangle + (v+u)|22\rangle] / \sqrt{2}, \quad (13)$$

where $|1\rangle$ and $|2\rangle$ are eigenstates of σ^x : $\sigma^x|1\rangle = |1\rangle$ and $\sigma^x|2\rangle = -|2\rangle$, and $|12\rangle$ denotes that the state of first qubit is $|1\rangle$ and that of second one is $|2\rangle$. The parameters u and v are given by

$$u = \frac{1}{\sqrt{2}} \sqrt{1 + (V-K)/W}, \quad v = \frac{1}{\sqrt{2}} \sqrt{1 - (V-K)/W}, \quad (14)$$

where $W = \sqrt{\eta^2 \Delta^2 + (V-K)^2}$. Thus, the qubit dependent part of H'_0 may be diagonalized as

$$\begin{aligned} H'_0 = & -W (|A\rangle\langle A| - |D\rangle\langle D|) - (V-K) (|B\rangle\langle B| - |C\rangle\langle C|) \\ & + \sum_k \omega_k b_k^\dagger b_k - V + F\sigma_0^2/4, \end{aligned} \quad (15)$$

and U_ϵ in Eq. (5) becomes

$$U_\epsilon = -\epsilon' \{ (u|A\rangle + v|D\rangle)\langle B| + |B\rangle(u\langle A| + v\langle D|) \}. \quad (16)$$

In this work we consider only the case of weak bias with $\epsilon/\omega_c \leq 10^{-5}$ [1]. At the lowest order of ϵ we can diagonalize $H'_0 + U_\epsilon$ in the space expanded by $|A\rangle$ and $|B\rangle$,

$$|A\rangle = \cos\theta|G\rangle - \sin\theta|X\rangle, \quad |B\rangle = \sin\theta|G\rangle + \cos\theta|X\rangle, \quad (17)$$

where

$$\begin{aligned} \cos\theta = & \frac{1}{\sqrt{2}} \left(1 + \frac{W-V+K}{\Sigma} \right)^{1/2}, \quad \sin\theta = \frac{1}{\sqrt{2}} \left(1 - \frac{W-V+K}{\Sigma} \right)^{1/2}, \\ \Sigma = & \sqrt{(W-V+K)^2 + 4\epsilon'^2 u^2}. \end{aligned} \quad (18)$$

Then we have

$$\begin{aligned}
H'_0 + U_\epsilon = & -\frac{1}{2}[W + V - K + \Sigma]|G\rangle\langle G| - \frac{1}{2}[W + V - K - \Sigma]|X\rangle\langle X| \\
& + (V - K)|C\rangle\langle C| + W|D\rangle\langle D| + \sum_k \omega_k b_k^\dagger b_k - V + F\sigma_0^2/4 \\
& - \epsilon'v \{(-\sin\theta|G\rangle + \cos\theta|X\rangle)\langle D| + h.c.\}.
\end{aligned} \tag{19}$$

It is easy to see that if the last term in Eq. (19) is neglected, the ground state of $H'_0 + U_\epsilon$ is $|G\rangle$, and in this work we are mainly concerned with the ground state properties. In Eq. (19), the coefficient of the transition term $|G\rangle\langle D| + |D\rangle\langle G|$ is $\epsilon'v \sin\theta \propto \epsilon'^2$. In numerical calculations we use a very small bias $\epsilon'/\omega_c \leq 10^{-5}$ to trigger the QPT [1] while staying in the range of $\epsilon'/\omega_c \leq 0.05$, and consequently, the transition term $|G\rangle\langle D| + |D\rangle\langle G|$ can be dropped safely. Fortunately, the QCP at $\alpha \sim \alpha_c$ falls within this range, and our numerical calculations are carried out in the range of $0 \leq \alpha \leq 1.1\alpha_c$.

The first-order Hamiltonian H'_1 can be recast as

$$\begin{aligned}
H'_1 = & \sum_k g_k b_k^\dagger \left\{ (1 - \xi_k) \left[u(\cos\theta|G\rangle - \sin\theta|X\rangle)(\sin\theta\langle G| + \cos\theta\langle X|) + h.c. - \frac{\sigma_0}{2} \right] \right. \\
& + \frac{\eta\Delta}{\omega_k} \xi_k [v(\cos\theta|G\rangle - \sin\theta|X\rangle)(\sin\theta\langle G| + \cos\theta\langle X|) - h.c.] \left. \right\} + h.c. \\
= & \sum_k g_k (b_k^\dagger + b_k)(1 - \xi_k) \left[u \sin(2\theta)(|G\rangle\langle G| - |X\rangle\langle X|) - \frac{\sigma_0}{2} \right] \\
& + \sum_k g_k b_k^\dagger \left[u(1 - \xi_k) \cos(2\theta)(|G\rangle\langle X| + |X\rangle\langle G|) + v \frac{\eta\Delta}{\omega_k} \xi_k (|G\rangle\langle X| - |X\rangle\langle G|) \right] + h.c.,
\end{aligned} \tag{20}$$

where $h.c.$ is short for the Hermitian conjugate. Then, if we choose

$$\sigma_0 = 2u \sin(2\theta) = \frac{4u^2\epsilon'}{\Sigma}, \quad \xi_k = \frac{\omega_k}{\omega_k + \Sigma}, \tag{21}$$

we have $H'_1|G\rangle|\{0_k\}\rangle = 0$, where $|\{0_k\}\rangle$ is the vacuum state of the environment. Now we can see clearly the reason why we introduce the term $(1 - \xi_k)\sigma_0$ in Eq.(2) for the generator S . Note that the term $\xi_k(\sigma_1^z + \sigma_2^z)$ in S comes from the Silbey-Harris type ansatz where $\xi_k = \omega_k/(\omega_k + \Sigma) \approx 1$ for the high-frequency oscillators. However, $1 - \xi_k = \Sigma/(\omega_k + \Sigma) \approx 1$ for the lower-frequency oscillators and this is to say that when $\sigma_0 \neq 0$ the lower-frequency oscillators may play an important role. We will see

in next section that away from the QPT ($\alpha < \alpha_c$) we have $\sigma_0 \approx 0$ and the dynamic displacement in S , $\xi_k(\sigma_1^z + \sigma_2^z)$, dominates; but around the QCP $\alpha \sim \alpha_c$, $\sigma_0 \neq 0$ and the static displacement $(1 - \xi_k)\sigma_0$ comes into play.

Since $H'_1|G\rangle|\{0_k\}\rangle = 0$, the ground state of $H'_0 + U_\epsilon + H'_1$ is $|G\rangle|\{0_k\}\rangle$ with the ground state energy,

$$E_g = -\frac{1}{2}[W + V - K + \Sigma] - V + \sum_k \frac{g_k^2}{4\omega_k}(1 - \xi_k)^2\sigma_0^2. \quad (22)$$

This ground state energy can also be derived from the variational principle. Our theory is to introduce a trial ground state of the original Hamiltonian H (Eq.(1)),

$$|g.s.\rangle = \exp(-S)|G\rangle|\{0_k\}\rangle. \quad (23)$$

The ground state energy is Eq.(22):

$$E_g = \langle g.s. | H | g.s. \rangle = \langle \{0_k\} | \langle G | \exp(S) H \exp(-S) | G \rangle | \{0_k\} \rangle$$

(Note that $\langle \{0_k\} | \langle G | H'_2 | G \rangle | \{0_k\} \rangle = 0$). If $\sigma_0 = 0$, our ground state is the same as the variational ground state of Ref.[13]. But for $\alpha \geq \alpha_c$, we introduce a finite σ_0 which can be determined by the ground state variation: $\partial E_g / \partial \sigma_0 = 0$. It is easily to prove that $\partial E_g / \partial \sigma_0 = 0$ leads to Eq.(21) for σ_0 . We will show in next section that a nonzero σ_0 leads to a nonzero $\langle \sigma_z \rangle \neq 0$ which determines the QCP.

Furthermore, the ground state average of σ^x is

$$\langle \sigma_1^x \rangle_G = \langle \sigma_2^x \rangle_G = \frac{1}{2} \langle g.s. | (\sigma_1^x + \sigma_2^x) | g.s. \rangle = \frac{\eta^2 \Delta}{W} \cos^2 \theta. \quad (24)$$

The numerical results of E_g and $\langle \sigma^x \rangle_G$ will be shown in next section.

III Quantum phase transition

We use the same criterion as that used in Ref.[1] to determine the critical coupling in this work, that is, the emergence of a non-zero ground state expectation of $\langle \sigma^z \rangle$ as the coupling α increases across some critical point α_c . We note that this criterion

is different from that of Ref.[13], where the vanishing of the renormalized tunneling $\eta \rightarrow 0$ is used as the criterion. Since $\epsilon' = \epsilon + F\sigma_0$, Eq. (21) leads to

$$\sigma_0 = \frac{4u^2\epsilon}{\Sigma} \left/ \left(1 - \frac{4u^2F}{\Sigma} \right) \right. . \quad (25)$$

The ground state average of σ^z is

$$\langle \sigma_1^z \rangle_G = \langle \sigma_2^z \rangle_G = \frac{1}{2} \langle G | (\sigma_1^z + \sigma_2^z) | G \rangle = u \sin(2\theta) = \frac{2\epsilon' u^2}{\Sigma} = \frac{\sigma_0}{2}. \quad (26)$$

As $\epsilon/\omega_c < 10^{-5}$ is very small, Eq.(18) leads to $\Sigma \approx W - V + K$ for the delocalized phase. In this phase $\sigma_0 \sim \epsilon$ is also very small until

$$1 - \frac{4u^2F}{W - V + K} = 0, \quad (27)$$

where a quantum phase transition occurs, and a finite average $\langle \sigma_1^z \rangle = \langle \sigma_2^z \rangle$ emerges. That is, the two-qubit SBM exhibits two ground state phases [1]: a delocalized phase in which $\langle \sigma_{1,2}^z \rangle \rightarrow 0$ in the limit of $\epsilon \rightarrow 0$, and a localized phase with $\langle \sigma_{1,2}^z \rangle \neq 0$ even in the presence of an infinitesimal bias $\epsilon = 0^+$. Note that σ_0 (Eq.(25)) is not divergent at the transition point and in the localized phase because $1 - 4u^2F/\Sigma > 0$ (Σ is defined in Eq.(18)) and $\epsilon' > 0$ even if $\epsilon = 0^+$.

The critical coupling strength at the QCP α_c can be determined by Eq. (27) because $F \propto \alpha$. For effectively ferromagnetic coupling ($K - V < 0$) in the zeroth-order Hamiltonian H'_0 of Eq. (4), it is found that $W - V + K \approx 0.5\eta^2\Delta^2/(V - K)$ in the scaling limit of $\Delta \ll \omega_c$, and to the lowest order of Δ/ω_c , we have

$$F = 2\alpha\omega_c^{1-s} \int_0^{\omega_c} \frac{(W - V + K)^2 \omega^{s-1} d\omega}{(\omega + W - V + K)^2} \sim \frac{2\pi\alpha\omega_c(1-s)}{\sin[\pi(1-s)]} \left\{ \frac{W - V + K}{\omega_c} \right\}^s. \quad (28)$$

Then, Eq. (27) becomes

$$1 - \frac{4\pi\alpha_c(1-s)(W + V - K)}{\sin[\pi(1-s)]W} \left(\frac{W - V + K}{\omega_c} \right)^{s-1} = 0. \quad (29)$$

When $K < V$ and $\Delta \ll \omega_c$, $W - V + K \approx 0.5\eta^2\Delta^2/(V - K)$ and $(W + V - K)/W \approx 2$. Then, it is easily seen that $\alpha_c = 1/8 + O(\Delta/\omega_c)$ for $s = 1$, and $\alpha_c = 0 + O(\Delta/\omega_c)$ for $s < 1$. In the super-Ohmic regime of $s > 1$, $\alpha_c \rightarrow \infty$, and the system is always in

the delocalized state in the limit of $\epsilon \rightarrow 0$. Our estimation is comparable to those of Ref. [1]: $\alpha_c = 0.15 + \mathcal{O}(\Delta/\omega_c)$ for $s = 1$ and $\alpha_c = 0 + \mathcal{O}(\Delta/\omega_c)$ for $s < 1$. Moreover, it is also interesting to list the prediction of Ref. [13]: $\alpha_c = 0.5$ for $s = 1$.

For finite values of Δ/ω_c , the QCP can be determined by Eq. (27). Figure 1 is the α -versus- Δ phase diagram for various values of s with $K = 0$ and very weak bias $\epsilon/\omega_c = 10^{-5}$. One can see that in the scaling limit $\Delta/\omega_c \rightarrow 0$, $\alpha_c \rightarrow 0.125$ for the Ohmic bath $s = 1$, and $\alpha_c \rightarrow 0$ for the sub-Ohmic bath $s < 1$. Meanwhile, α_c increases with increasing tunneling Δ because a larger tunneling strength favors the delocalized state.

Figure 2 is the α -versus- K phase diagram for various values of s with $\Delta/\omega_c = 0.1$ and very weak bias $\epsilon/\omega_c = 10^{-5}$, which is similar to Figs. 2 and 3 in Ref.[1]. As the effective Ising interaction in H'_0 is $(K - V)\sigma_1^z\sigma_2^z$, a positive (antiferromagnetic) K reduces the bath-induced interaction $-V$, while a negative (ferromagnetic) K enhances it. This explains that in the phase diagram a positive K favors the delocalized phase while a negative K is unfavorable to it. One can see that the phase boundary depends on K very weakly for the ferromagnetic case ($K < 0$), while for the antiferromagnetic case ($K > 0$) the delocalized region extends to a larger α_c , and the asymptotic line of the phase boundary for a larger $K > 0$ is given by $K_r = K - \alpha\Omega_c/s = 0$ (K_r is the renormalized Ising coupling defined by Ref. [1]). We present a comparison of the NRG results and ours in Figs. 2(b) (Ohmic bath) and 2(c) (sub-Ohmic bath). For $K < 0$, the phase boundary of α_c for the Ohmic bath is weakly dependent on K , which is the same as the NRG results. However, the boundary, located at $\alpha_c = 1/8 + \mathcal{O}(\Delta/\omega_c)$, is also weakly dependent on Δ , a result at variance with the NRG counterpart of $\alpha_c = 0.15 + \mathcal{O}(\Delta/\omega_c)$. For the sub-Ohmic bath, our calculated α_c is in good agreement with that of the NRG approach for the whole range of K values.

Figure 3(a) shows the difference in the ground state energy between our calculation and that in [13] in the presence of an Ohmic bath ($s = 1$). For the delocalized phase $\alpha < \alpha_c$, our E_g is the same as that of Ref. [13]. However, above the transition point $\alpha \geq \alpha_c$, the lower ground state energy indicates that the ansatz of this work is a better one for the real ground state. As shown in the figure the calculated value of the

parameter σ_0 , is nearly zero for the delocalized phase ($\alpha < \alpha_c$), but increases quickly above the transition point.

Figure 3(b) shows the ground state average of $\langle \sigma^x \rangle$ and the renormalized bias ϵ' as functions of α for an Ohmic bath. One can see that our calculated average $\langle \sigma^x \rangle$ (see Eq.(24)) is the same as that of Ref. [13] for $\alpha < \alpha_c$, and in this regime, the renormalized bias $\epsilon' \approx \epsilon$ is very small, while for $\alpha \geq \alpha_c$, ϵ' increases quickly. Since our interest is mainly on the QCP, our calculation is restricted to the parameter regime of $0 < \alpha \leq 1.1\alpha_c$ where $\epsilon'/\omega_c < 0.05$ and the transition term $|G\rangle\langle D| + |D\rangle\langle G|$ in Eq.(19) can be safely neglected.

Eqs. (25) and (26) are used to get the ground state averages of $\langle \sigma^z \rangle = \langle \sigma_1^z \rangle = \langle \sigma_2^z \rangle$ as a function of ϵ , α , Δ , or K . As critical exponents are the most interesting QPT properties, we first consider a critical exponent δ defined by

$$\langle \sigma^z \rangle \sim \epsilon^{1/\delta}, \quad (30)$$

where α , Δ , and K are kept fixed at their critical values. Fig. 4 shows a log-log plot of the relation between $\langle \sigma^z \rangle$ and ϵ/ω_c for $\Delta/\omega_c = 0.1$ and $K = 0$, and $\alpha = \alpha_c$. A series of s values are taken. The filled blue dots in Fig. 2 indicate the transition points in the phase diagram where we cross the phase boundary to calculate the curves in Fig. 4. One can see the power-law scaling over more than two orders of magnitude, and the critical exponent δ can be determined from simply fitting the slope. The fitting results are listed in the second column of Table 1, which are in the close vicinity of $\delta = 3$.

Second, the static susceptibility is related to the critical exponent γ ,

$$\chi = \left. \frac{\langle \sigma^z \rangle}{\epsilon} \right|_{\epsilon \rightarrow 0} \sim \frac{1}{(\alpha_c - \alpha)^\gamma}, \quad (31)$$

where Δ and K are kept fixed. Figure 5 shows a log-log plot of the relation between χ and $\alpha_c - \alpha$ for various values of s (the transition points are again the filled blue dots in Fig. 2). There is a power-law scaling and the critical exponent γ can be determined from simply fitting the slope. The fitting results, which are listed in the third column of Table 1, are found to be quite close to the value of $\gamma = 1$.

Another three critical exponents are defined as follows,

$$\langle \sigma^z \rangle \sim (\alpha - \alpha_c)^\beta, \quad (32)$$

$$\langle \sigma^z \rangle \sim (\Delta_c - \Delta)^{\beta'}, \quad (33)$$

$$\langle \sigma^z \rangle \sim (K_c - K)^\zeta. \quad (34)$$

They can be determined in the similar way, that is, by simply fitting the slope in a log-log plot and the results are listed in the fourth (transition points are filled blue dots in Fig. 2), fifth (transition points are filled blue dots in Fig. 1), and sixth (transition points are red circles in Fig. 2) columns of Table 1. All these fitted exponents are found to be close to $1/2$.

We have checked that these extracted exponents are independent of the position in the phase diagram where the phase boundaries are crossed. We note that our transformed Hamiltonian $H'_0 + U_\epsilon$ is a two-site Ising model in both the transverse ($\eta\Delta$) and longitudinal (ϵ') field. For the lattice Ising model (one-, two-, and three-dimensional) in transverse field it is well-known that there is a quantum phase transition when the transverse field changes across some critical value[18]. It was proved that the critical exponents of the d-dimensional Ising model in transverse field are the same as those of the classical Ising model (without the transverse field) in (d+1)-dimension. In mean-field approximation the critical exponents of the quantum Ising model (in transverse field) are $\delta = 3$, $\gamma = 1$, and $\beta = 1/2$, which are independent of the lattice dimension and the coordination number, and different from the exact analytic solution (for one-dimension) and numerical exact solutions (Monte Carlo, renormalization group, etc.). Note that these mean-field critical exponents are the same as our values for the two-qubit SBM. This is an indication that our theory for the QPT of the two-qubit SBM is a mean-field theory, that is, the effect of quantum fluctuations has been taken into account by a self-consistent mean-field.

Here we explain briefly how our mean-field approximation works. The two-qubit system and the heat bath are decoupled by the unitary transformation and in the generator S of the transformation we introduce two “mean-field” displacement of oscillators: (1) the dynamic displacement $\xi_k(\sigma_1^z + \sigma_2^z)$ related to the high-frequency oscillators since

$\xi_k \approx 1$ for large ω_k , which modifies the original tunneling $\Delta \rightarrow \eta\Delta$ (Eq. (8)) and renormalizes the Ising coupling $K \rightarrow K - V$ (Eq. (9)); (2) the static displacement $(1 - \xi_k)\sigma_0$ related to the lower-frequency oscillators as $1 - \xi_k \approx 1$ for $\omega_k \rightarrow 0$, which leads to the modified bias $\epsilon \rightarrow \epsilon'$ (Eq. (5)). As shown above, self-consistent calculations have been carried out to determine these modified parameters and to include the effect of the quantum fluctuations.

Moreover, all the critical exponents listed in Table 1 are independent of the bath index s and this is a feature similar to the mean-field exponents of the quantum Ising model which are independent of the dimension and the coordination number. We note that, for $s = 1/2$, our critical exponents are the same as the scaling analysis result of Ref.[1].

As for the critical exponents, our results come from a self-consistent mean-field ground state. It leads reasonably to s -independent plain mean-field critical exponents. In contrast, the critical exponents of the mean-field analysis in Ref. [1] is based on the quantum to classical mapping of the spin-boson model to the one-dimensional classical Ising model with long-range interaction $J_{ij} = J/|i - j|^{1+s}$, which results in the s -dependent critical exponents. On the other hand, as pointed out in Ref. [1], the NRG is not well suited to describe the system close to the transition for $s < 1/2$, and the calculation is therefore restricted to $s \geq 1/2$. It is our belief that it is not accidental that the critical exponents $\zeta(s = 1/2) = 1/2$ and $\beta(s = 1/2) = 0.5$ of the NRG are equivalent to those of our theory. Recent Quantum Monte Carlo simulation yields classical exponents of $\gamma = 1$ and $\beta = 0.5$ for $s < 1/2$ in a multi-qubit SBM[14], but for $s > 1/2$, their critical exponents are dependent on s while ours are independent of s .

IV The entanglement entropy

The reduced system density matrix ρ_S is given by tracing the total (system + bath) density operator over the boson bath: $\rho_S = \text{Tr}_B[\rho_{SB}]$. If the ground-state reduced density matrix of the two-qubit system ρ_S is known, the von Neumann entanglement

entropy can be calculated from ρ_S : $\mathcal{E} = -\text{Tr}[\rho_S \log_2 \rho_S]$ [19, 1]. From the trial ground state (24) we have

$$\rho_{SB} = |g.s.\rangle\langle g.s.| = \exp(-S)|G\rangle|\{0_k\}\rangle\langle\{0_k\}| \langle G| \exp(S). \quad (35)$$

Thus,

$$\rho_S = \text{Tr}_B\{\exp(-S)|G\rangle|\{0_k\}\rangle\langle\{0_k\}| \langle G| \exp(S)\}. \quad (36)$$

Note that there are both the spin operators σ^z and the bosonic operators $b_k^\dagger - b_k$ in S . For the trace operation over the bath (Tr_B) we use Eqs. (17), (18), (10), (11) and $|1\rangle = (|\uparrow\rangle + |\downarrow\rangle)/\sqrt{2}$, $|2\rangle = (|\uparrow\rangle - |\downarrow\rangle)/\sqrt{2}$ ($|\uparrow\rangle(|\downarrow\rangle)$ is the eigenstate of σ^z : $\sigma^z|\uparrow(\downarrow)\rangle = +(-)|\uparrow(\downarrow)\rangle$) to express $|G\rangle$ as

$$\begin{aligned} |G\rangle &= \cos\theta|A\rangle + \sin\theta|B\rangle \\ &= \frac{1}{\sqrt{2}}\{(u\cos\theta + \sin\theta)|\uparrow\uparrow\rangle + (u\cos\theta - \sin\theta)|\downarrow\downarrow\rangle + v\cos\theta[|\uparrow\downarrow\rangle + |\downarrow\uparrow\rangle]\}. \end{aligned} \quad (37)$$

Then,

$$\begin{aligned} \exp(-S)|G\rangle &= \frac{1}{\sqrt{2}}(u\cos\theta + \sin\theta)\exp(-S_+)|\uparrow\uparrow\rangle \\ &+ \frac{1}{\sqrt{2}}(u\cos\theta - \sin\theta)\exp(-S_-)|\downarrow\downarrow\rangle + v\cos\theta\exp(-S_0)\frac{1}{\sqrt{2}}[|\uparrow\downarrow\rangle + |\downarrow\uparrow\rangle], \end{aligned} \quad (38)$$

where

$$S_+ = \sum_k (f_k + \frac{g_k \xi_k}{\omega_k})(b_k^\dagger - b_k), \quad S_- = \sum_k (f_k - \frac{g_k \xi_k}{\omega_k})(b_k^\dagger - b_k), \quad S_0 = \sum_k f_k \omega_k (b_k^\dagger - b_k), \quad (39)$$

and $f_k = g_k(1 - \xi_k)\sigma_0/2\omega_k$. Now there are no system operators in S_+ , S_- and S_0 so that the cyclic properties of the trace can be used for trace operation in Eq. (36),

$$\rho_S = \begin{pmatrix} \frac{1}{2}(u\cos\theta + \sin\theta)^2 & \frac{v\eta}{\sqrt{2}}\cos\theta(u\cos\theta + \sin\theta) & \frac{1}{2}(u^2\cos^2\theta - \sin^2\theta)\eta^4 & 0 \\ \frac{v\eta}{\sqrt{2}}\cos\theta(u\cos\theta + \sin\theta) & v^2\cos^2\theta & \frac{v\eta}{\sqrt{2}}\cos\theta(u\cos\theta - \sin\theta) & 0 \\ \frac{1}{2}(u^2\cos^2\theta - \sin^2\theta)\eta^4 & \frac{v\eta}{\sqrt{2}}\cos\theta(u\cos\theta - \sin\theta) & \frac{1}{2}(u\cos\theta - \sin\theta)^2 & 0 \\ 0 & 0 & 0 & 0 \end{pmatrix}. \quad (40)$$

Because of the decoupling of the “dark” state $\frac{1}{\sqrt{2}}[|\uparrow\downarrow\rangle - |\downarrow\uparrow\rangle]$, all elements of the density operator ρ_S in the bottom row and right column are 0. If we know the three eigenvalues of the upper left 3×3 sub-matrix then the entanglement entropy is,

$$\mathcal{E} = - \sum_{i=1}^3 \lambda_i \log_2 \lambda_i, \quad (41)$$

where λ_i ($i = 1, 2, 3$) are the eigenvalues of the 3×3 sub-matrix. As the trace of the density operator is $\text{Tr}_S \rho_S = 1$, it is easy to prove that $0 \leq \mathcal{E} \leq 2[1]$. $\mathcal{E} = 0$ indicates the absence of entanglement between the qubits and the bath.

The eigenvalues of ρ_S can be calculated numerically. The entanglement entropy \mathcal{E} for the Ohmic case of $s = 1$ is shown in Fig. 6(a) as a function of the coupling strength α for three values of tunneling Δ (we set $K = 0$ and $\epsilon/\omega_c = 10^{-6}$). When $\alpha = 0$ there is no entanglement between qubits and environment and $\mathcal{E} = 0$. The entanglement entropy increases with increasing α in the delocalized phase, reaches a plateau and then drops quickly to zero at the transition point $\alpha = \alpha_c$ (Here and in the following figures our calculation is restricted to the range $0 < \alpha \leq 1.1\alpha_c$ because in this range $\epsilon'/\omega_c < 0.05$ and the transition term $|G\rangle\langle D| + |D\rangle\langle G|$ in Eq.(19) can be safely dropped). As pointed out in Ref. [1], the plateau indicates that coherence is lost prior to localization, that is, it shows that the system is in the coherent to incoherent crossover before final trapping in the localized phase.

Figure 6(b) displays the entanglement entropy \mathcal{E} for the sub-Ohmic case of $s = 1/2$ and three values of tunneling Δ (we set $K = 0$ and $\epsilon/\omega_c = 10^{-6}$). Obviously, for the sub-Ohmic bath the entanglement entropy reaches a sharp peak right at the transition point and there is no plateau corresponding to the coherent to incoherent crossover.

Figure 6(a) is corresponding to the case of $K = 0$, then the renormalized Ising coupling is $-V\sigma_1^z\sigma_2^z$. In Fig. 7 we check the \mathcal{E} versus α relation for finite values of the Ising coupling K ($s = 1$, $\Delta = 0.1$, $\epsilon/\omega_c = 10^{-6}$). From Fig. 7(a), we observe that as K changes from the ferromagnetic ($K < 0$) to the antiferromagnetic ($K > 0$, note that the renormalized Ising coupling is $K - V$) the width of the plateau is reduced considerably, and a spike emerges instead for large positive values for $K \geq 0.25\omega_c$. This indicates that the localization transition occurs right next to the regime where spin dynamics

is coherent [1], and coherence is lost in a manner similar to the sub-Ohmic case of Fig. 6(b). In Figs. 7(b) and 7(c), we show the comparison of the NRG results with ours. For several values of K , the slopes of our scaled data are similar to those of the NRG approach.

Figure. 8 shows the entanglement entropy \mathcal{E} as a function of α for various values of Ising coupling K in the sub-Ohmic regime of $s = 1/2$ (we set $\Delta = 0.1$ and $\epsilon/\omega_c = 10^{-6}$). There is a sharp peak at the transition point for both the ferromagnetic ($K < 0$) and the antiferromagnetic ($K > 0$) Ising coupling, but the width of the peak of the ferromagnetic coupling is much smaller than that of the antiferromagnetic one. In Figs. 8(b), 8(c), and 8(d), we show the comparison of the NRG results with ours. For several values of K , it is found that the slopes of our scaled data agree well with those of the NRG approach.

In Fig. 9 we show the \mathcal{E} versus α relations for $s = 1/4, 1/2, 3/4, 9/10$, and 1 (from left to right). Here we set Ising coupling $K = 0$. One can see that with increasing index s a sharp peak ($s = 1/4$) at the transition point changes gradually (with $s = 1/2, 3/4, 9/10$) to a plateau ($s = 1$) on the left side of the peak.

V Qubit-qubit correlation

In this section, in order to investigate the correlation between the two qubits mediated by the common bath and the effects of direct Ising couple, we calculate the qubit-qubit correlation function of the ground state. It is defined as

$$C_{12} = \langle \sigma_1^z \sigma_2^z \rangle - \langle \sigma_1^z \rangle \langle \sigma_2^z \rangle, \quad (42)$$

where $\langle \bullet \rangle = \langle g.s. | \bullet | g.s. \rangle$. By the reduced density matrix Eq. (38), we immediately arrive at

$$C_{12} = (u^2 - v^2) \cos^2 \theta + \sin^2 \theta - \frac{1}{4} \sigma_0^2. \quad (43)$$

In Fig. 10 we show the correlation function C_{12} for different bath indexes s . In Figs. 10(a) and 10(b), we show our calculated results and the data of the QMC simulations

for $K = 0$ [14]. Due to the coupling of the qubits and bath, there is an indirect Ising coupling $-V$. The function $\langle\sigma_1^z\sigma_2^z\rangle$ is nonzero even in the delocalized phase due to the effective ferromagnetic interaction mediated by the common bath. It is obvious to see that the fluctuation increases with the increase of the dissipative coupling before the QPT. At the critical point α_c , C_{12} is reached the maximum value, which means that the QPT happens. After passing α_c , C_{12} decreases rapidly. By comparison, our results are in good agreement with the QMC results, especially for the deep sub-Ohmic bath $s \leq 1/2$. In Fig. 10(a), for the Ohmic bath, our results of the delocalized phase agree well with the QMC data[14]. In Fig. 10(b), we notice that the transition of our results occurs at $\alpha_c = 0.133$ while that of the QMC happens at $\alpha \approx 0.175$.

In Figs. 10(c) and 10(d), we show the effects of direct Ising couple K on the correlation function for $s = 1$ and $s = 1/2$, respectively. For the Ohmic case the C_{12} has a character of plateau at the lower dissipation in the ferromagnetic case $K < 0$, while for larger values of K the plateau shrinks to a peaklike structure. It is clearly seen that the peak value of C_{12} for the antiferromagnetic situation is much higher than those for the ferromagnetic case. For the sub-Ohmic case $s = 1/2$, the C_{12} exhibits a character of cusp for any K , similar to the entanglement entropy in Fig. 8(a).

VI Discussion and conclusion

We have proposed an ansatz to study a two-qubit system interacting with a dissipative environment in the ground state, and it is shown that, as a result of the competition between the intrasite tunneling and the intersite correlation, a quantum phase transition to the localized phase may occur at some critical coupling constant α_c . By calculating the ground state entanglement entropy between the qubits and the bath as well as the qubit-qubit correlation function, we have explored the nature of the QPT between the delocalized and localized state.

The same criterion as that used in Ref.[1] is used to determine the critical coupling in this work, that is, the emergence of a non-zero ground state expectation of $\langle\sigma^z\rangle$ as the coupling α increases across some critical point α_c . For the two-qubit system

in Ohmic bath we get $\alpha_c = 1/8 + O(\Delta/\omega_c)$ which is quite close to the NRG result $\alpha_c = 0.15 + O(\Delta/\omega_c)$ [1]. But the criterion used in Ref.[13] is the vanishing of the renormalized tunneling $\eta \rightarrow 0$, which leads to $\alpha_c = 0.5$ for the two-qubit system in Ohmic bath. However, for the single-qubit system in Ohmic bath both the criteria $\eta \rightarrow 0$ and $\langle \sigma^z \rangle \neq 0$ give the same critical value $\alpha_c = 1$, at least in the scaling limit $\Delta/\omega_c \rightarrow 0$ (Refs.[2-12]). This difference comes from the two-qubit correlation and the renormalized Ising coupling V (Eq.(9)) which shift the QCP of the two-qubit SBM substantially as compared to that of the single-qubit case.

A new unitary transformation has been utilized, in which a ω_k -dependent function ξ_k is introduced and the functional form of it is determined by setting zero the matrix element of H'_1 between the ground state and the lowest-lying excited state of $H'_0 + U_\epsilon$. Then we get the ground state $|G\rangle|\{0_k\}\rangle$ for the transformed Hamiltonian $H'_0 + U_\epsilon + H'_1$ ($H'_1|G\rangle|\{0_k\}\rangle = 0$) with the ground state energy Eq. (22). Generally speaking, our approach is to decouple the two-qubit system from the heat bath by the unitary transformation with the generator S (Eq.(2)). In S we introduce two “mean-field” displacement of oscillators: (1)The dynamic displacement $\xi_k(\sigma_1^z + \sigma_2^z)$ related to the high-frequency oscillators since $\xi_k \approx 1$ for large ω_k , which modifies the original tunneling $\Delta \rightarrow \eta\Delta$ (Eq. (8)) and renormalizes the Ising coupling $K \rightarrow K - V$ (Eq. (9)). (2)The static displacement $(1 - \xi_k)\sigma_0$ related to the lower-frequency oscillators as $1 - \xi_k \approx 1$ for $\omega_k \rightarrow 0$, which leads to the modified bias $\epsilon \rightarrow \epsilon'$ (Eq. (5)). Self-consistent mean-field calculations have been carried out to determine these modified parameters, then the effect of the quantum fluctuations is included. Our calculated critical exponents are the same as the mean-field critical exponents of the Ising model in transverse field.

In our work, the unperturbed part of the transformed Hamiltonian $H'_0 + U_\epsilon$ can be solved exactly, but nonetheless contains the main physics of the two-qubit SBM. For the ground state the first-order Hamiltonian H'_1 can be neglected because $H'_1|G\rangle|\{0_k\}\rangle = 0$. The main approximation in our treatment is the omission of H'_2 (Eq. (7)). The reason to justify this approximation is that, since $\langle\{0_k\}|\langle G|H'_2|G\rangle|\{0_k\}\rangle = 0$ (because of the definition for η (Eq.(8)), the terms in H'_2 are related to the multi-boson non-diagonal

transitions (like $b_k b_{k'}$ and $b_k^\dagger b_{k'}^\dagger$). The contributions of these non-diagonal terms to the ground state energy are $O(g_k^2 g_{k'}^2)$ and higher. For the ground state the contribution from these multi-boson non-diagonal transition may be dropped safely. We have made substantial arguments in our previous publication[15] that this omission is justified.

Acknowledgement

This work was supported by the National Natural Science Foundation of China (Grants No. 11174198 and 11374208), the National Basic Research Program of China (Grant No. 2011CB922200), and by the Singapore National Research Foundation under Project No. NRF-CRP5-2009-04.

References

- [1] P. P. Orth, D. Roosen, W. Hofstetter, and K. L. Hur, Phys. Rev. **B82**, 144423 (2010).
- [2] A. J. Leggett, S. Chakravarty, A. T. Dorsey, M. P. A. Fisher, A. Garg, and W. Zwerger, Rev. Mod. Phys. **59**, 1 (1987).
- [3] U. Weiss, *Quantum Dissipative Systems* (World Scientific, Singapore, 1999).
- [4] R. Bulla, N. H. Tong, and M. Vojta, Phys. Rev. Lett. 91, 170601 (2003).
- [5] R. Bulla, H. J. Lee, N. H. Tong, and M. Vojta, Phys. Rev. B 71, 045122 (2005); M. Vojta, N. H. Tong, and R. Bulla, Phys. Rev. Lett. 94, 070604 (2005); F. B. Anders, R. Bulla, and M. Vojta, Phys. Rev. Lett. 98, 210402 (2007); N. H. Tong and Y.H. Hou, Phys. Rev. B 85, 144425 (2012) .
- [6] K. L. Hur, P. Doucet-Beaupre, and W. Hofstetter, Phys. Rev. Lett. **99**, 126801 (2007).
- [7] A. Winter, H. Rieger, M. Vojta, and R. Bulla, Phys. Rev. Lett. **102**, 030601 (2009).

- [8] A. Alvermann and H. Fehske, Phys. Rev. Lett. 102, 150601 (2009).
- [9] Y. Zhang, Q.H. Chen, and K. Wang, Phys. Rev. **B81**, 121105 (2010); N. Wu, L. Duan, X. Li, and Y. Zhao, J. Chem. Phys. **138**, 084111 (2013).
- [10] Cheng Guo, Andreas Weichselbaum, Jan von Delft, and Matthias Voja Phys. Rev. Lett. 108, 160401 2012
- [11] R. Silbey and R. A. Harris, J. Chem. Phys. **80**, 2615 (1984).
- [12] H. Zheng and Z. Lü, J. Chem. Phys. **138**, 174117 (2013).
- [13] D. P. S. McCutcheon, A. Nazir, S. Bose, and A. J. Fisher, Phys. Rev. **B81**, 235321 (2010).
- [14] A. Winter and H. Rieger, Phys. Rev. B **90**, 224401 (2014).
- [15] C. Zhao, Z. Lü and H. Zheng, Phys. Rev. **E84**, 011114 (2011).
- [16] A. W. Chin, J. Prior, S. F. Huelga, and M. B. Plenio, Phys. Rev. Lett. **107** 160601 (2011).
- [17] N. Zhou L. Chen, Y. Zhao, D. Mozyrsky, V. Chernyak, and Y. Zhao, Phys. Rev. B **90**,155135 (2014).
- [18] R. B. Stinchcombe, J. Phys. C: Solid State Phys. **6**, 2459 (1973).
- [19] Y. Zhao, P. Zanardi, and G. Chen, Phys. Rev. B **70**, 195113 (2004).

Figure Captions

Fig. 1 α versus Δ phase diagram for various bath type with $K = 0$ and very weak bias $\epsilon/\omega_c = 10^{-5}$. The five curves from the top down are for $s = 1, 0.9, 0.75, 0.5$, and 0.25 , respectively. The blue dots indicate the positions where we cross the phase boundary for calculating the critical exponents β' in the fifth column of Table 1.

Fig. 2 (a) α versus K phase diagram for various bath type with $\Delta/\omega_c = 0.1$ and very weak bias $\epsilon/\omega_c = 10^{-5}$. The five curves from the top down are for $s = 1, 0.9, 0.75, 0.5$, and 0.25 , respectively. The blue dots indicate the positions where we cross the phase boundary for calculating the critical exponents in the second (δ), third (γ), and fourth (β) columns of Table 1. The red circles indicate the positions where we cross the phase boundary for calculating the critical exponents in the sixth column (ζ) of Table 1. The comparisons of our result and NRG one for $s = 1$ and $s = 1/2$ are shown in Figs. 2(b) and (c), respectively. Different red symbols stand for the NRG data in Ref. [1]. The black curves correspond to our calculated data by our ansatz. The short-dash dotted lines in Figs. (b) and (c) indicate $K_r = 0$.

Fig. 3(a) The solid line is the difference between our calculation of the ground state energy and that of [13] in the Ohmic bath $s = 1$ with $K = 0$, $\Delta/\omega_c = 0.1$ and $\epsilon/\omega_c = 10^{-5}$. The dashed-dotted line is the calculated value of the parameter σ_0 . The arrow at the right corner is to indicate the transition point $\alpha_c \approx 0.1338$.

Fig. 3(b) The ground state average of $\langle \sigma^x \rangle$ and the renormalized bias ϵ' as functions of α for Ohmic bath $s = 1$ with $K = 0$, $\Delta/\omega_c = 0.1$ and $\epsilon/\omega_c = 10^{-5}$. The solid line is our result for $\langle \sigma^x \rangle$ and the dashed line is that of Ref.[13]. The arrow at the right corner is to indicate the transition point $\alpha_c \approx 0.1338$.

Fig. 4 The log-log plot of the relation between $\langle \sigma^z \rangle$ and ϵ/ω_c for various bath type with fixed $\Delta/\omega_c = 0.1$, $K = 0$ at their corresponding critical values of $\alpha = \alpha_c$. $s = 1, 0.9, 0.75, 0.5$, and 0.25 (from top to bottom).

Fig. 5 The log-log plot of the relation between χ and $1/(\alpha_c - \alpha)^\gamma$ for various bath type with fixed $\Delta/\omega_c = 0.1$ and $K = 0$. $s = 1, 0.9, 0.75, 0.5$, and 0.25 (from top to bottom).

Fig. 6(a) The entanglement entropy \mathcal{E} as a function of dissipation α for the Ohmic case of $s = 1$ with different tunneling Δ ($K = 0$, $\epsilon/\omega_c = 10^{-6}$).

Fig. 6(b) The entanglement entropy \mathcal{E} as a function of dissipation α for the sub-Ohmic case of $s = 1/2$ with different tunneling Δ ($K = 0$, $\epsilon/\omega_c = 10^{-5}$).

Fig. 7 (a) The entanglement entropy \mathcal{E} as a function of α for different Ising coupling K in Ohmic bath $s = 1$ ($\Delta = 0.1$, $\epsilon/\omega_c = 10^{-5}$). The comparisons of the scaled entanglement entropy versus $(\alpha - \alpha_c)/\alpha_c$ for $K = 0$ and $4K = 0.5\omega_c$ are shown in (b) and (c), respectively.

Fig. 8 (a) The entanglement entropy \mathcal{E} as a function of α for deferent Ising coupling K in sub-Ohmic bath $s = 1/2$ ($\Delta = 0.1$, $\epsilon/\omega_c = 10^{-5}$). The comparisons of the scaled entanglement entropy versus $(\alpha - \alpha_c)/\alpha_c$ for $4K/\omega_c = -0.5, 0$ and 0.5 are shown in (b), (c), and (d), respectively.

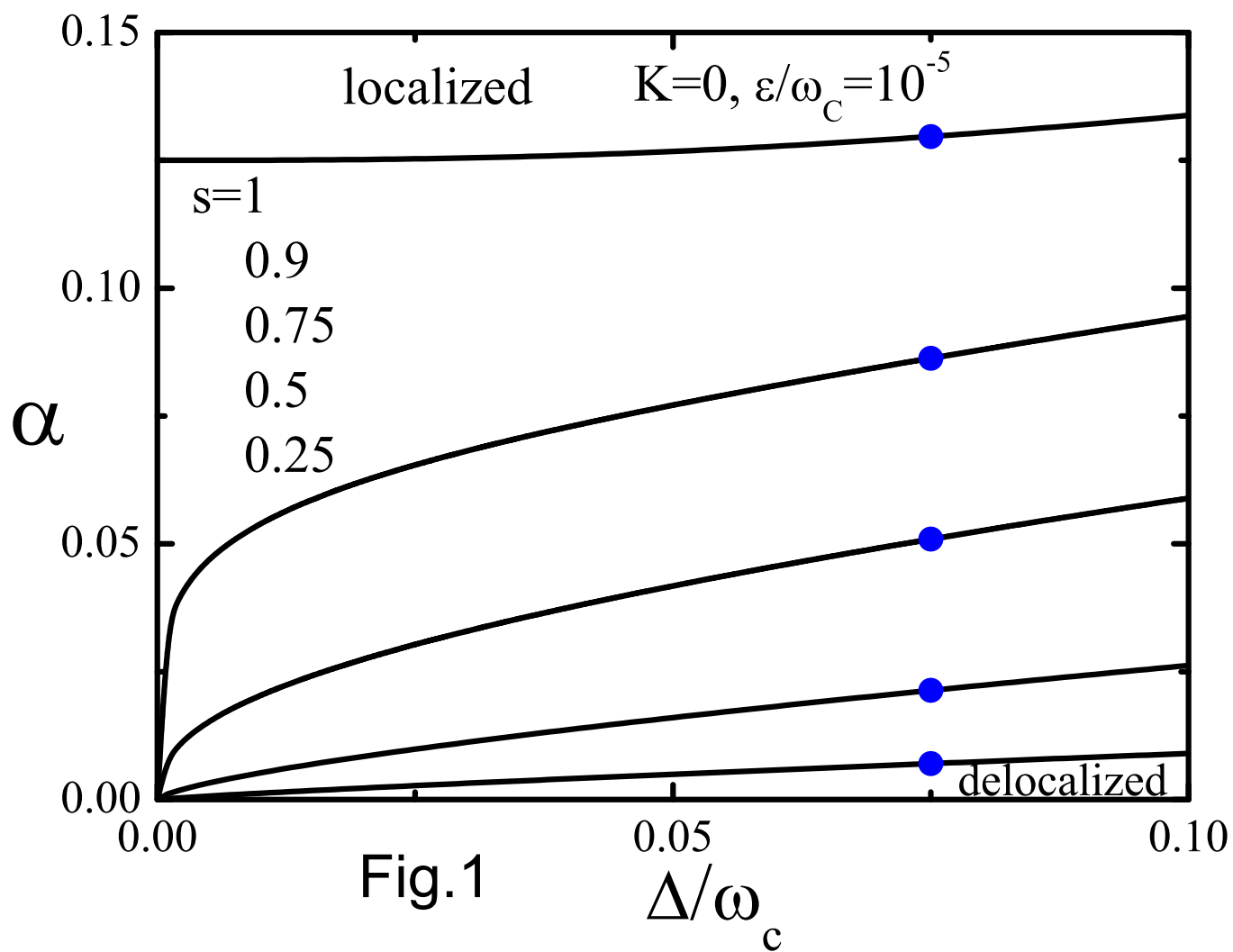
Fig. 9 The entanglement entropy \mathcal{E} as a function of α for the different bath index $s = 1/4, 1/2, 3/4, 9/10$, and 1 (from left to right).

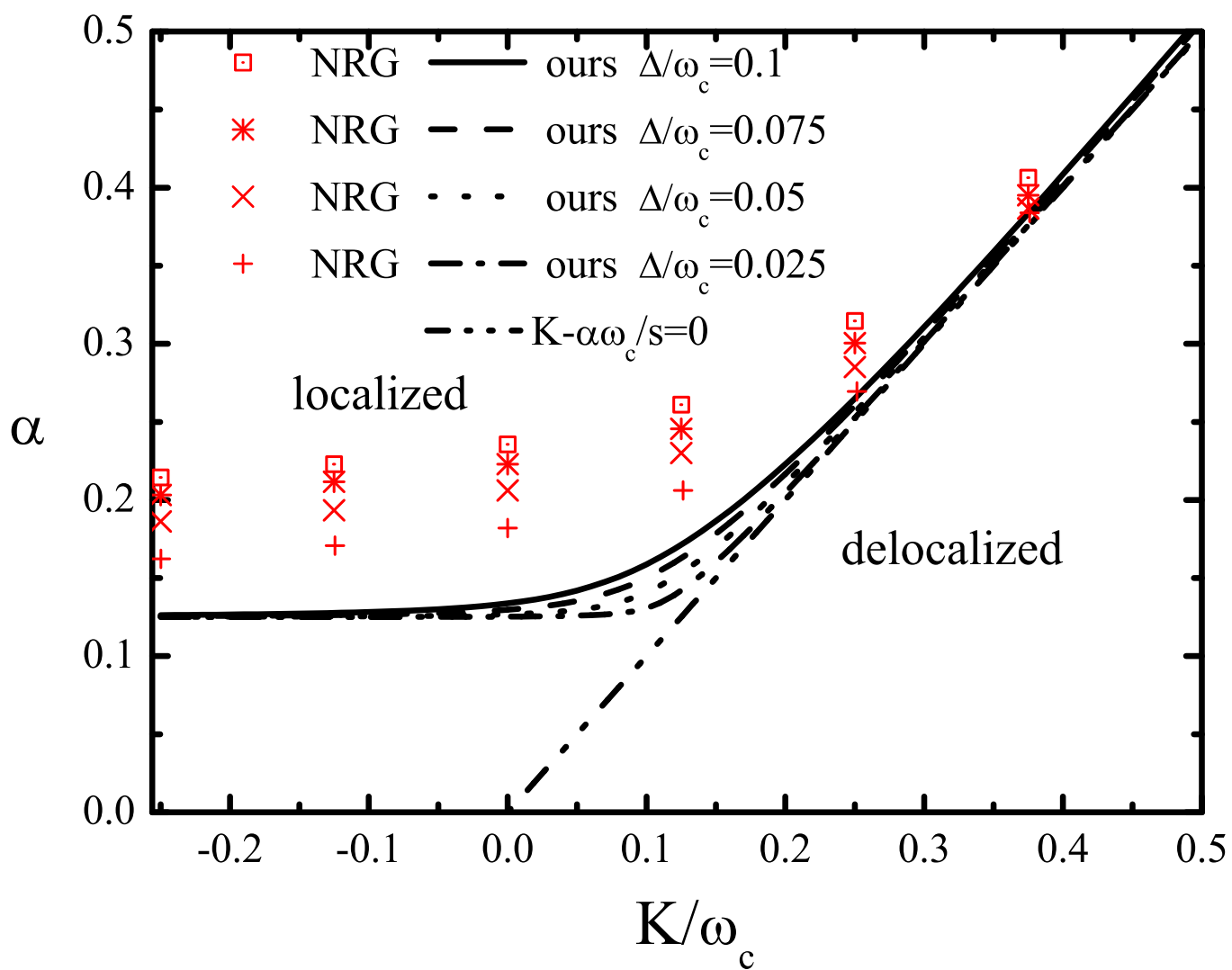
Fig. 10 (a) The qubit-qubit correlation function C_{12} as a function of α for Ising coupling $K = 0$ with different bath indexes $s = 0.25, 0.5, 0.75$, and 1 ($\Delta = 0.1$, $\epsilon/\omega_c = 10^{-5}$). The data of Quantum Monte Carlo in Ref.[14] are shown for comparison. (b) C_{12} versus α for $K = 0$ in the Ohmic case. The correlation functions C_{12} for $s = 1$ and $s = 1/2$ are shown in (c) and (d), respectively. Different curves are for different values of the Ising coupling K .

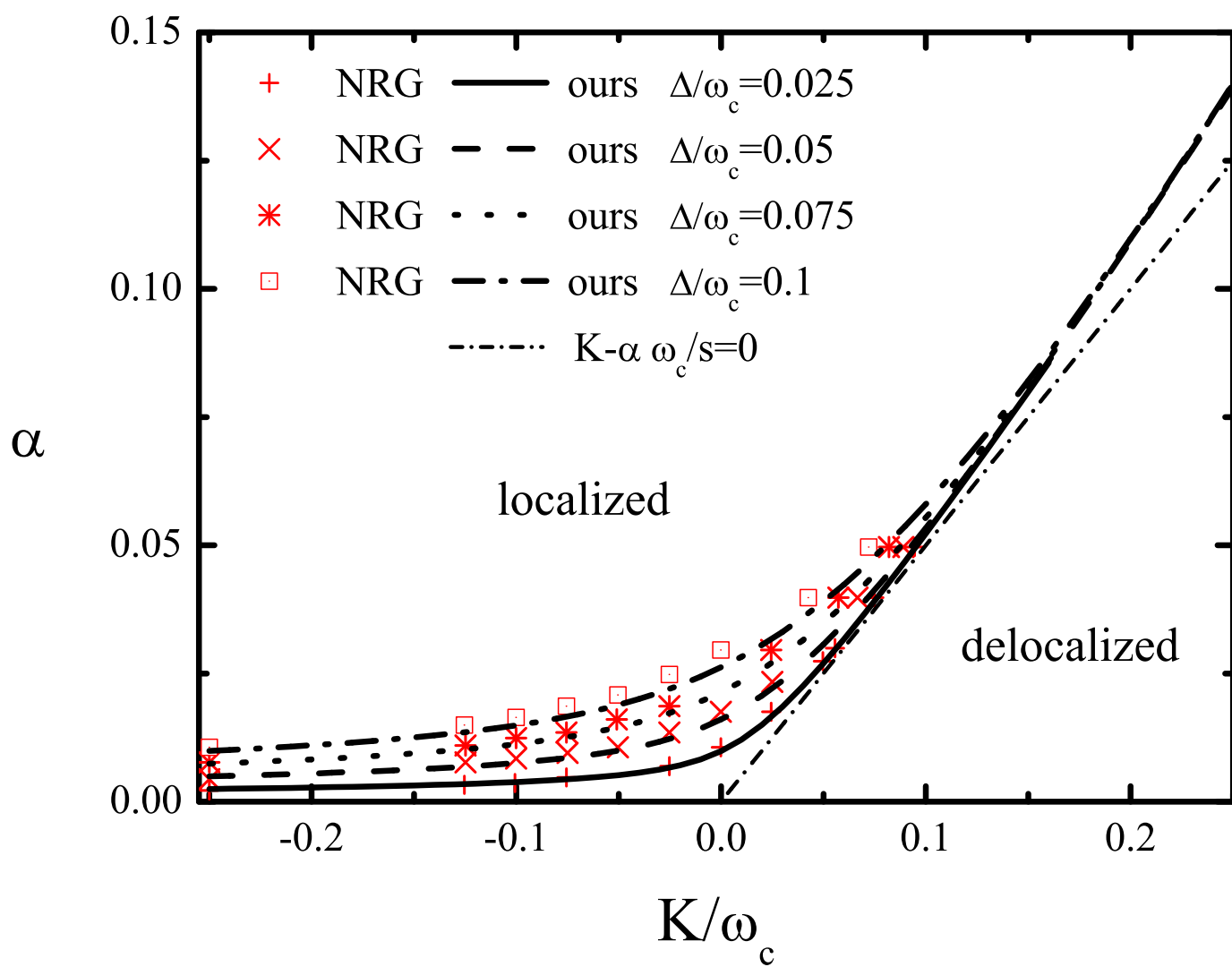
Tables

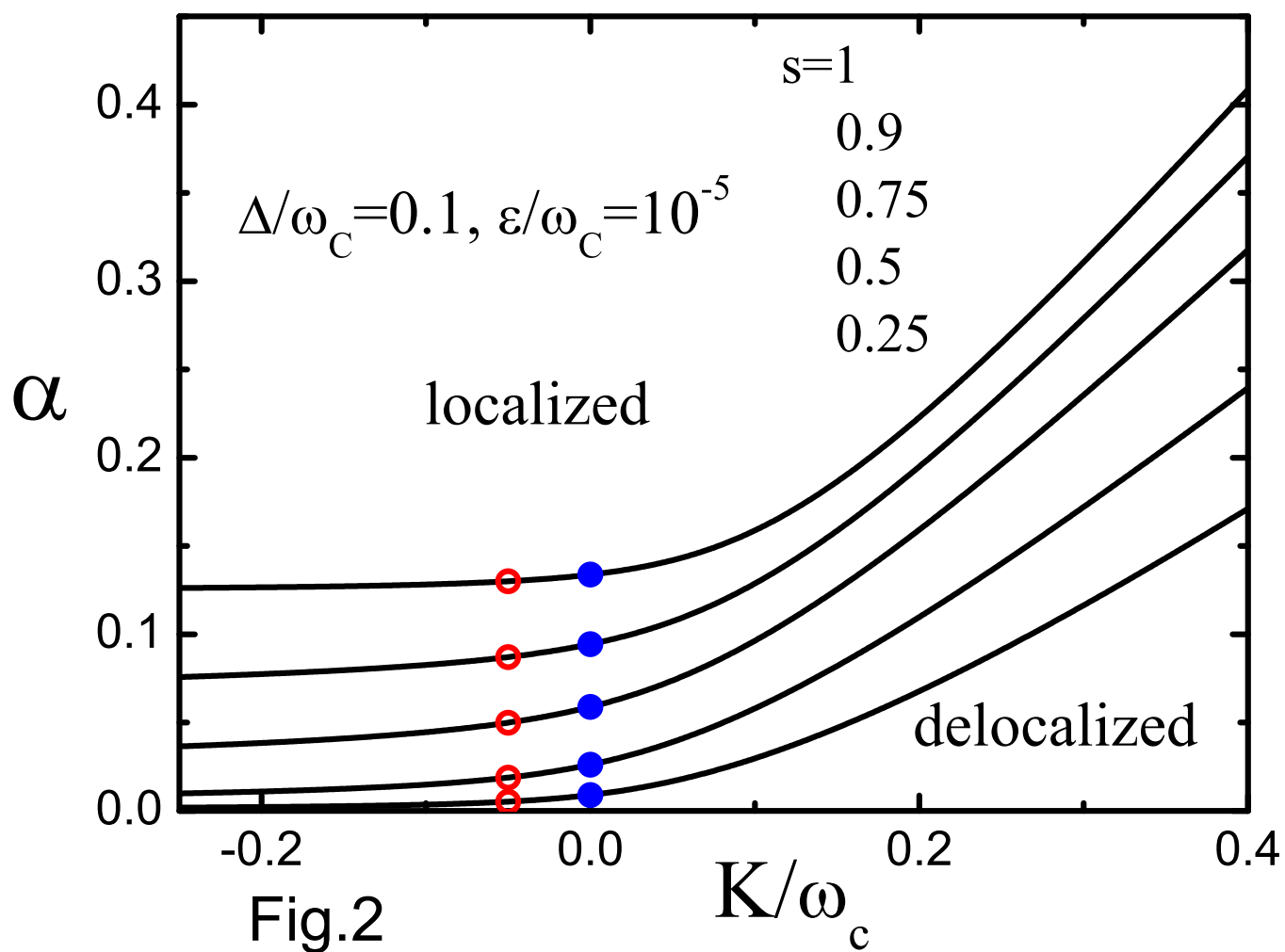
Table 1 Critical exponents of different bath type s .

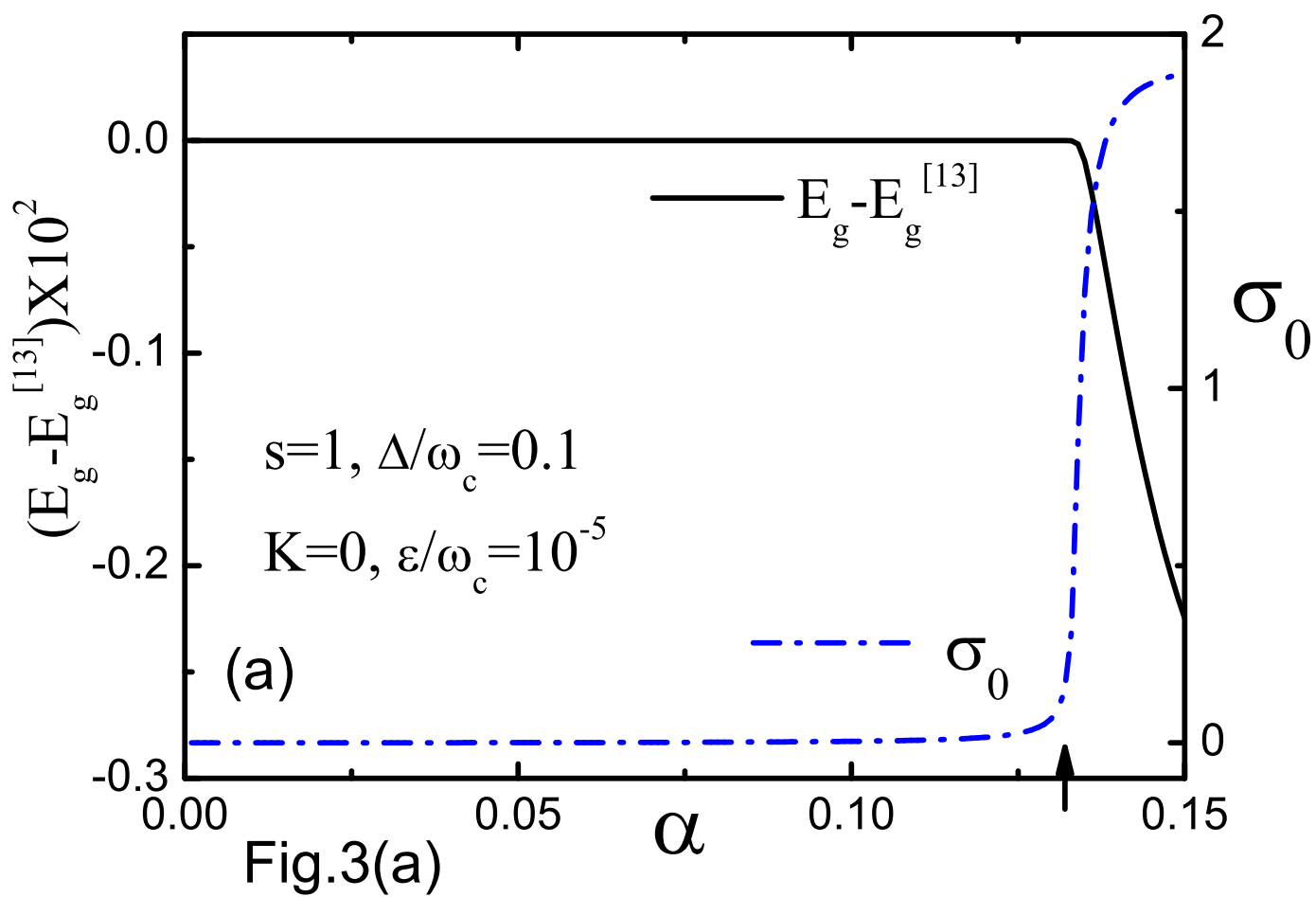
s	δ	γ	β	β'	ζ
0.25	3.0009	0.99999	0.49695	0.49988	0.49981
0.5	3.0015	1.00009	0.49848	0.49981	0.49979
0.75	3.0036	1.00041	0.49882	0.49971	0.49980
0.9	3.0088	1.00004	0.49864	0.49960	0.49979
1	3.0396	0.99999	0.49538	0.49912	0.49965

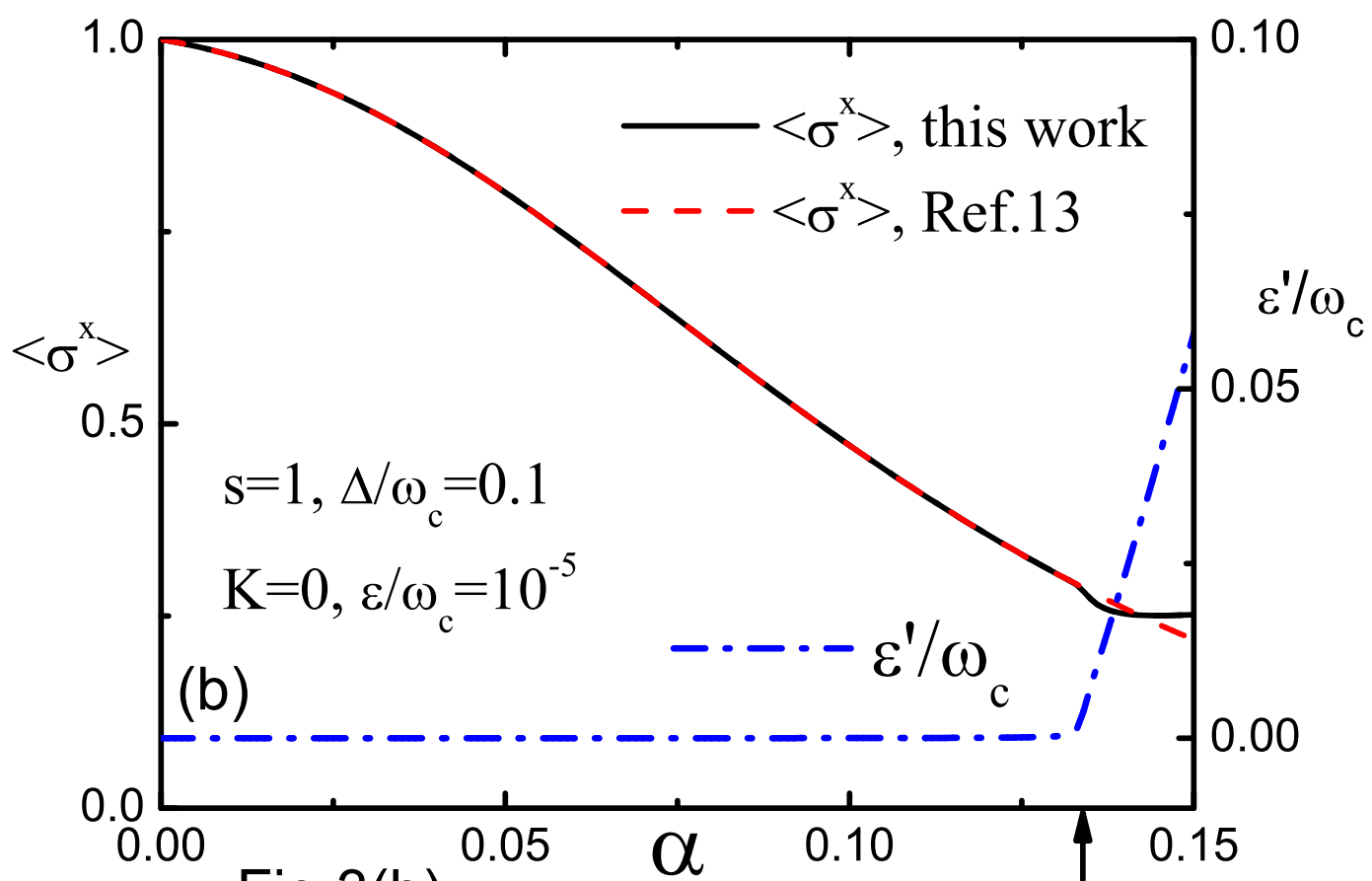


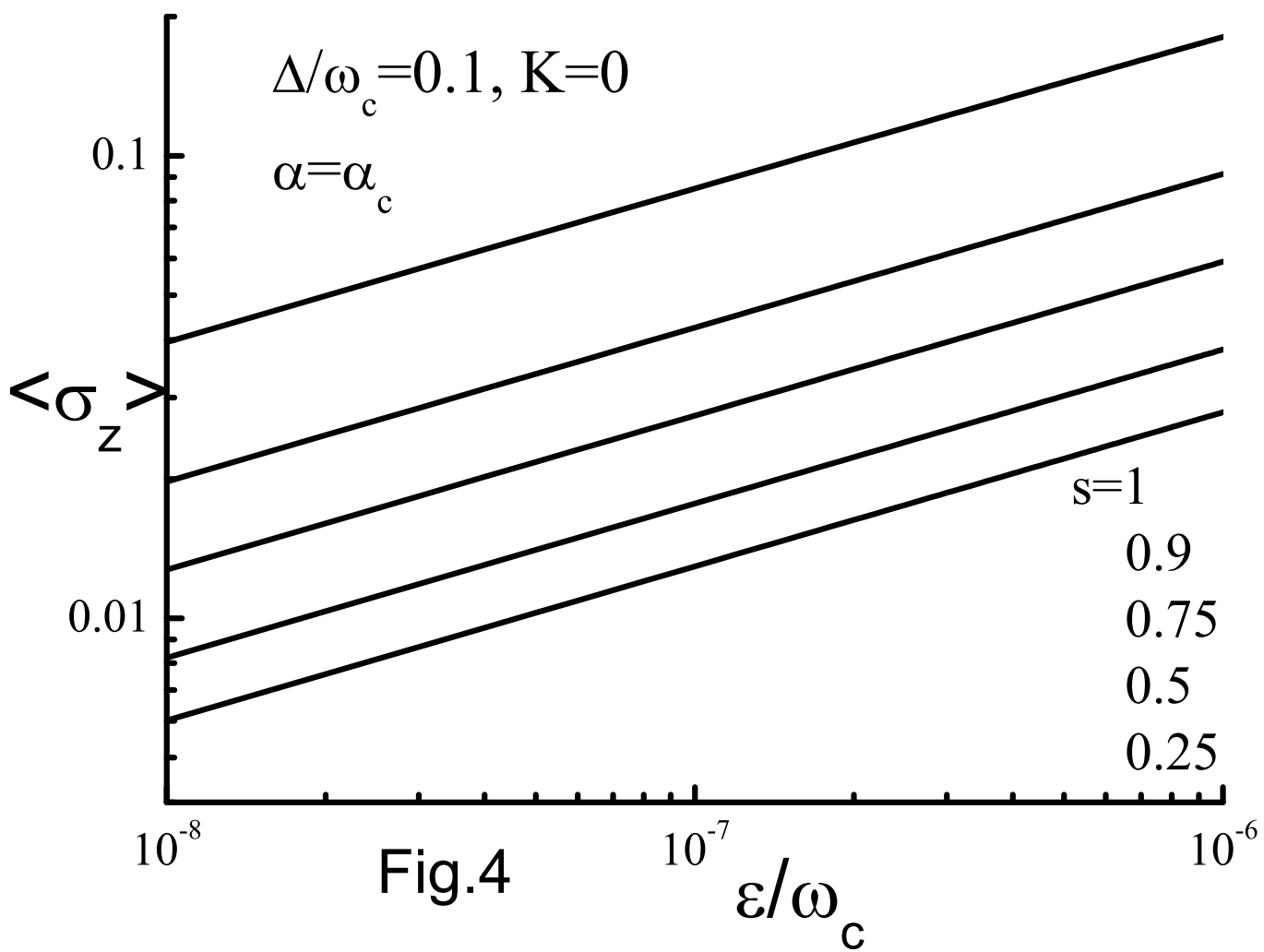












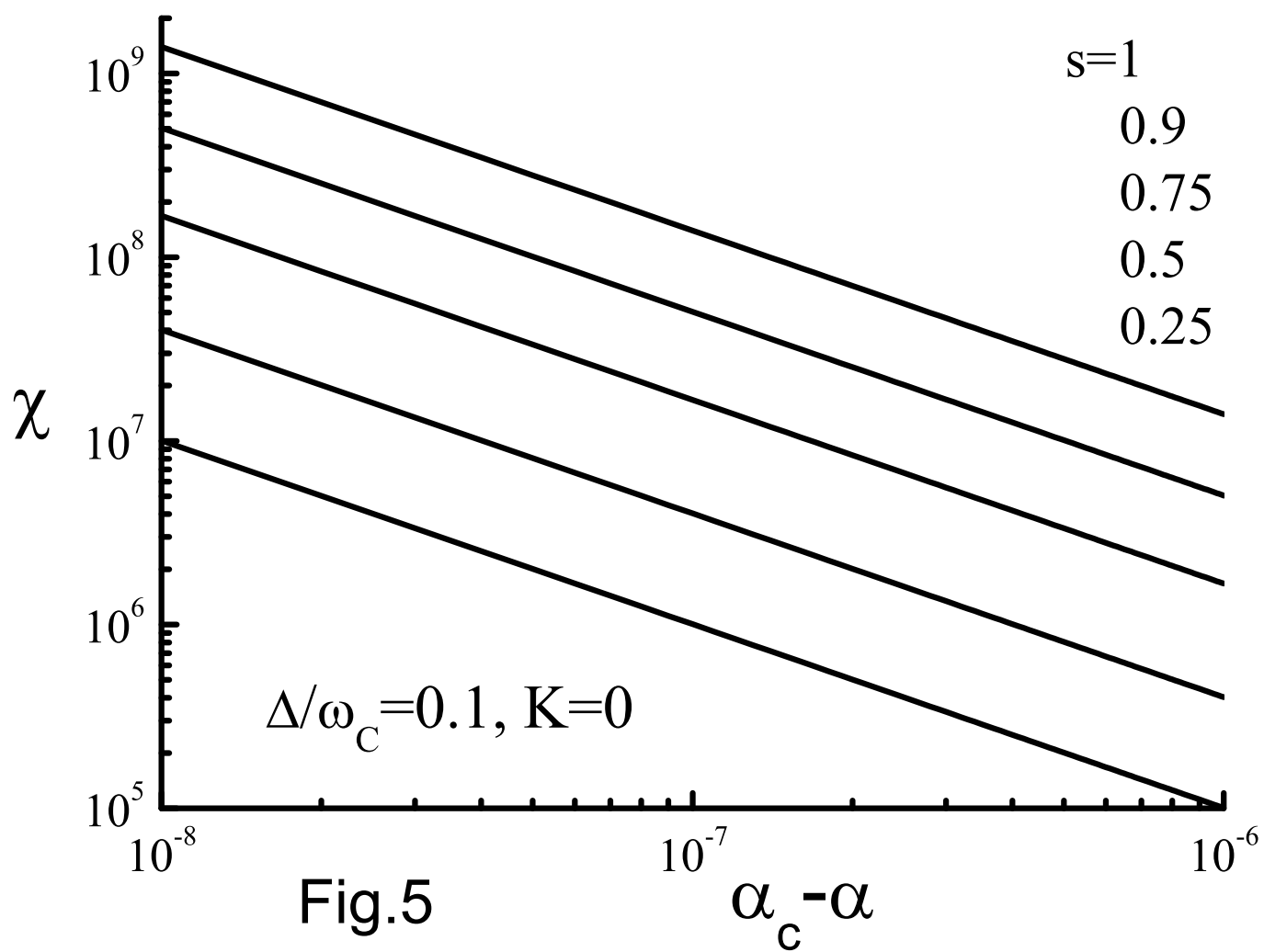


Fig.5

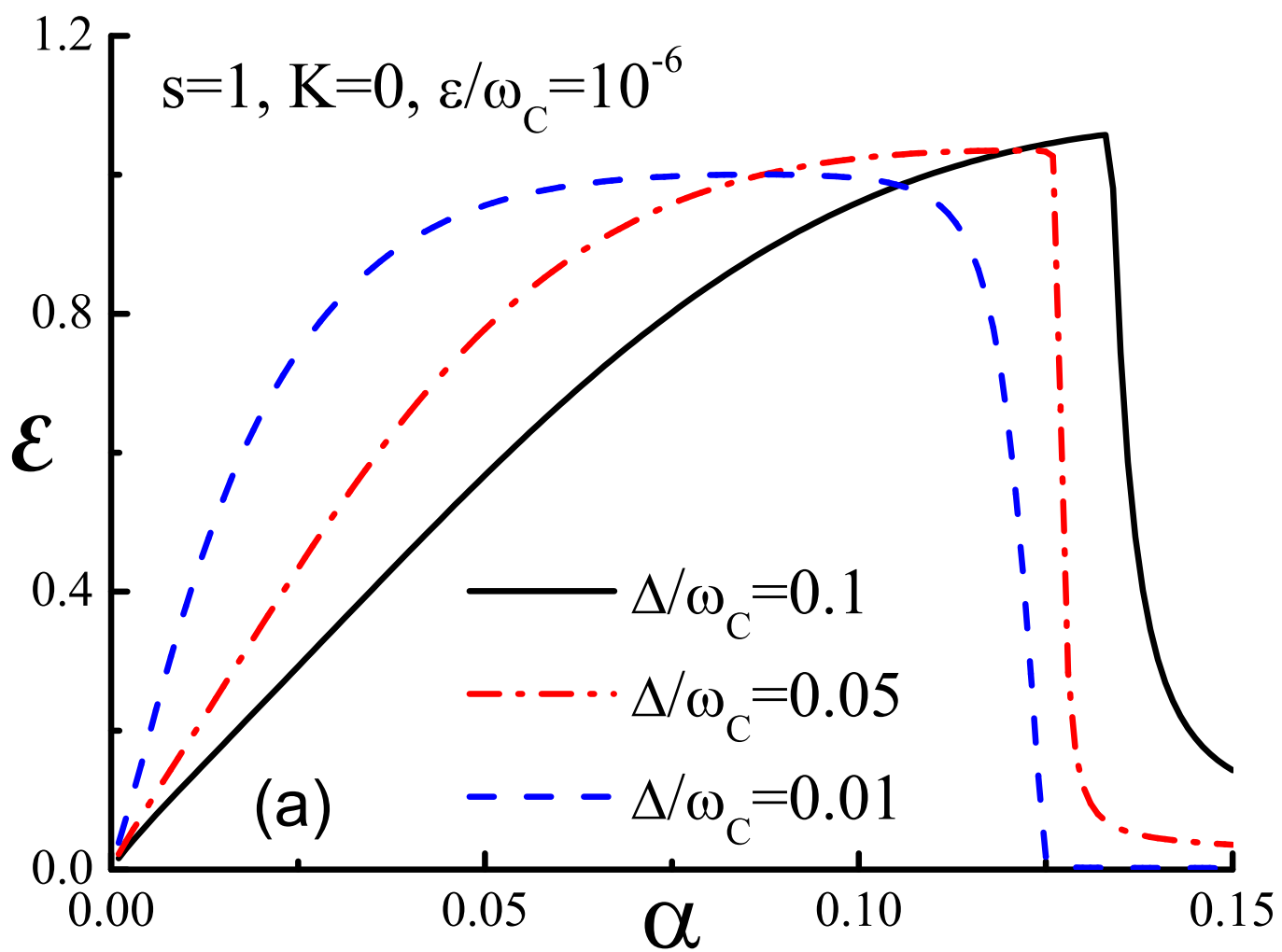
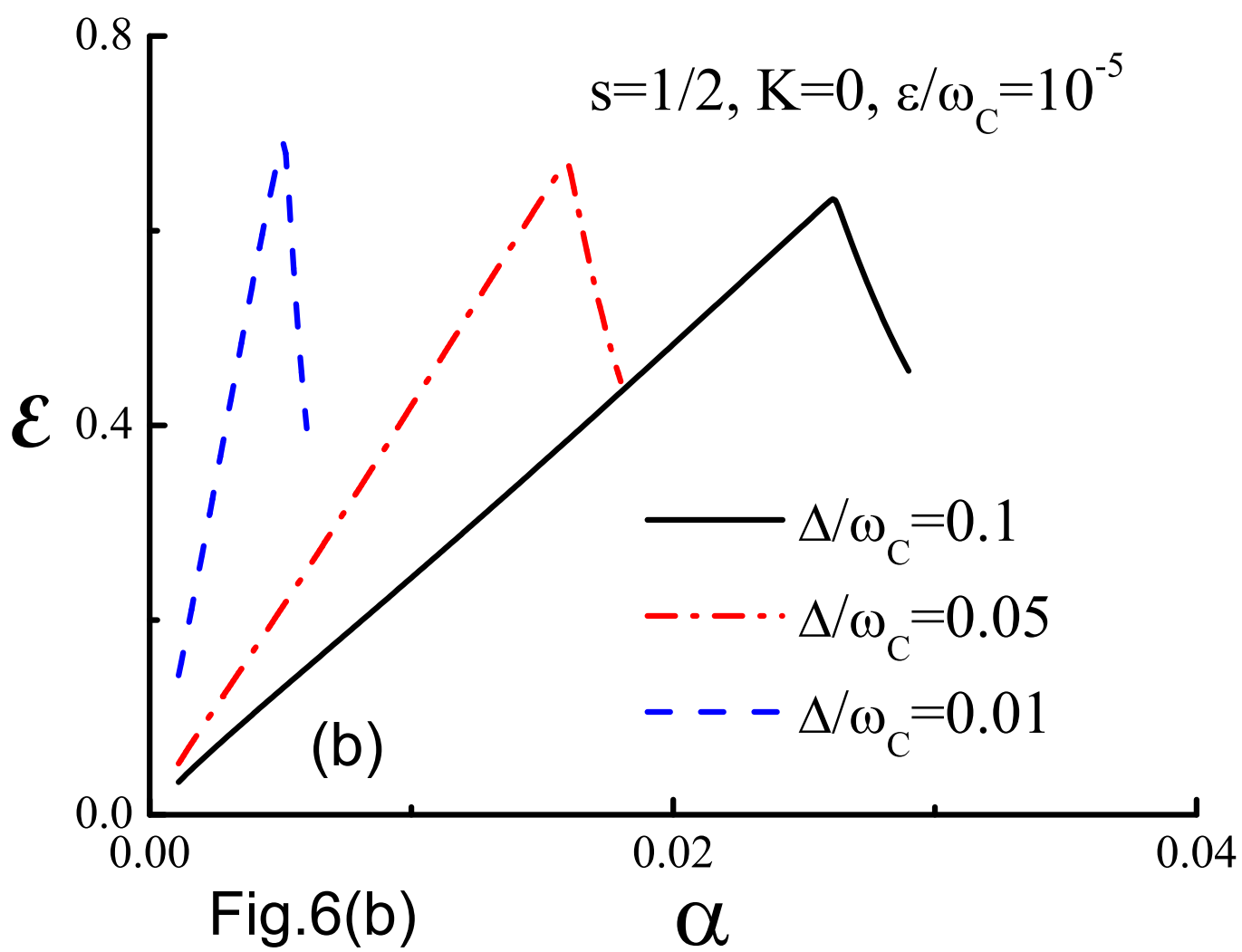
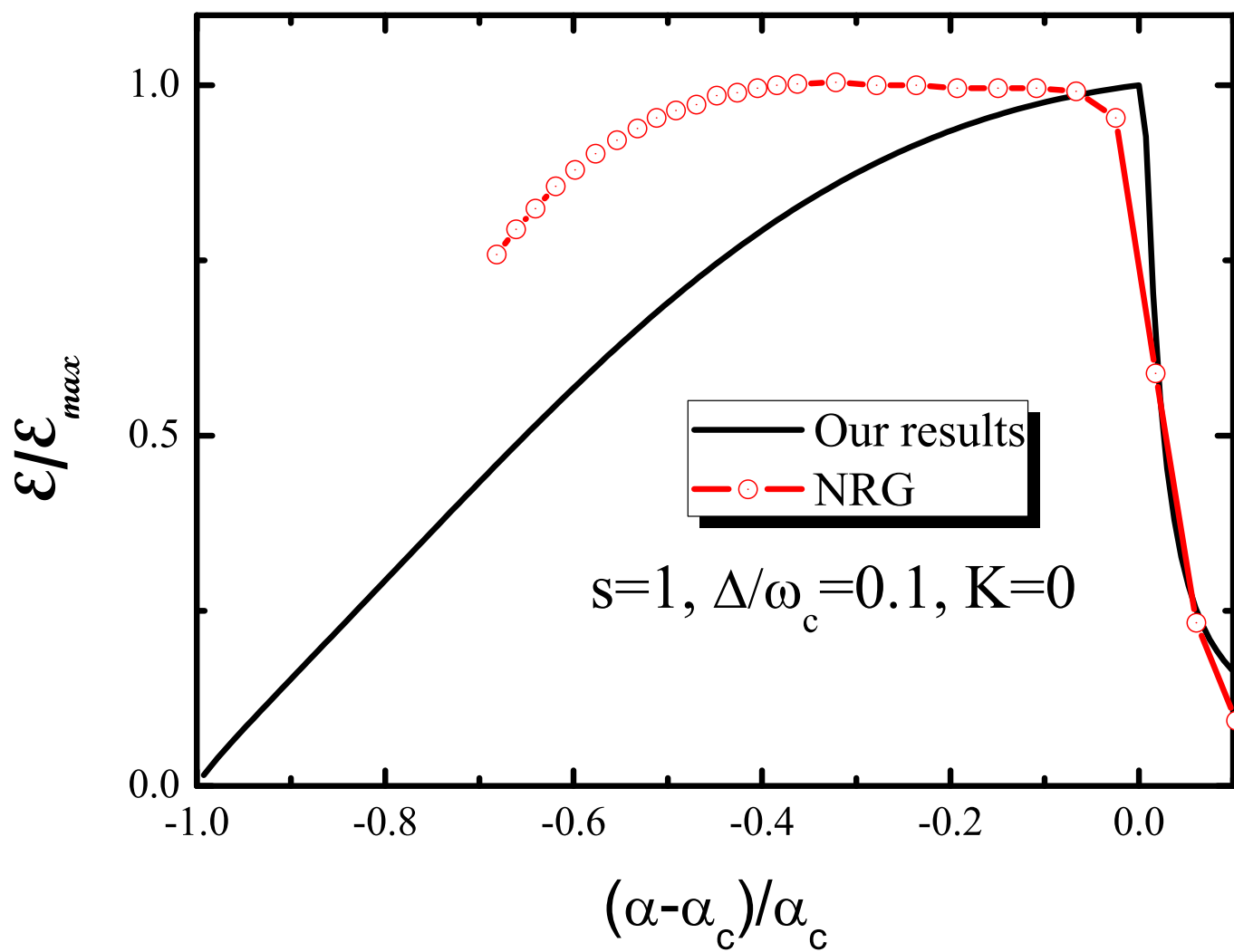
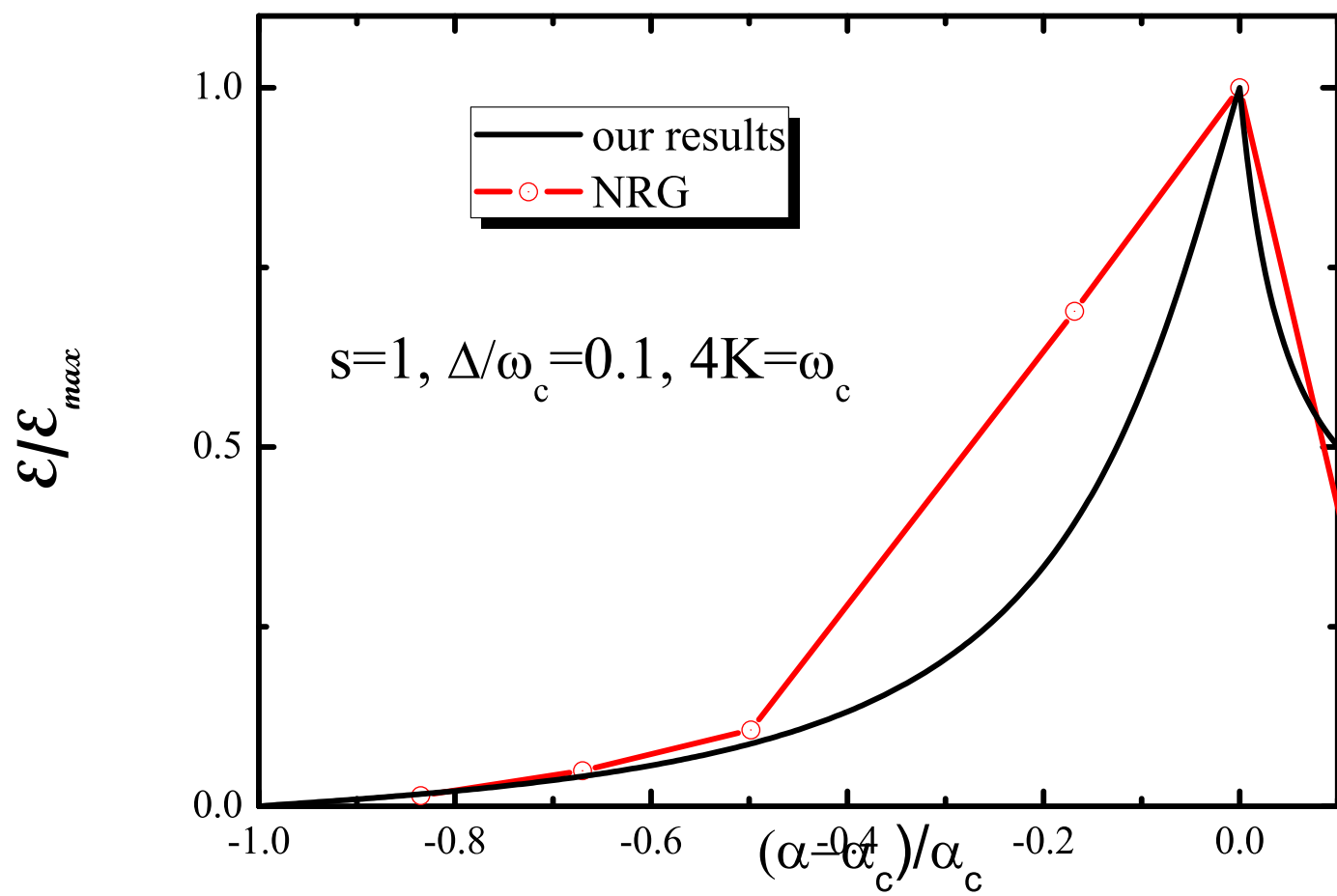
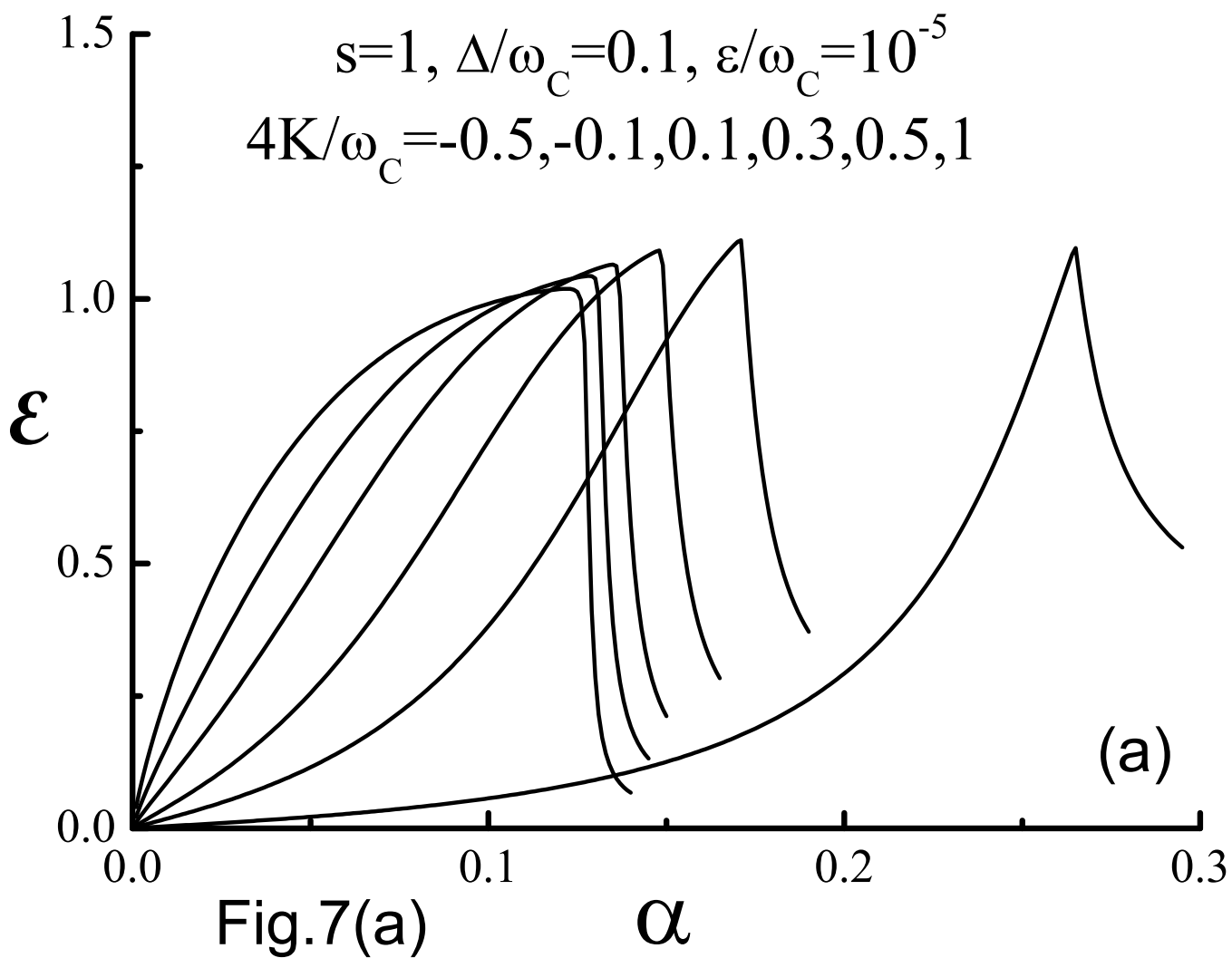


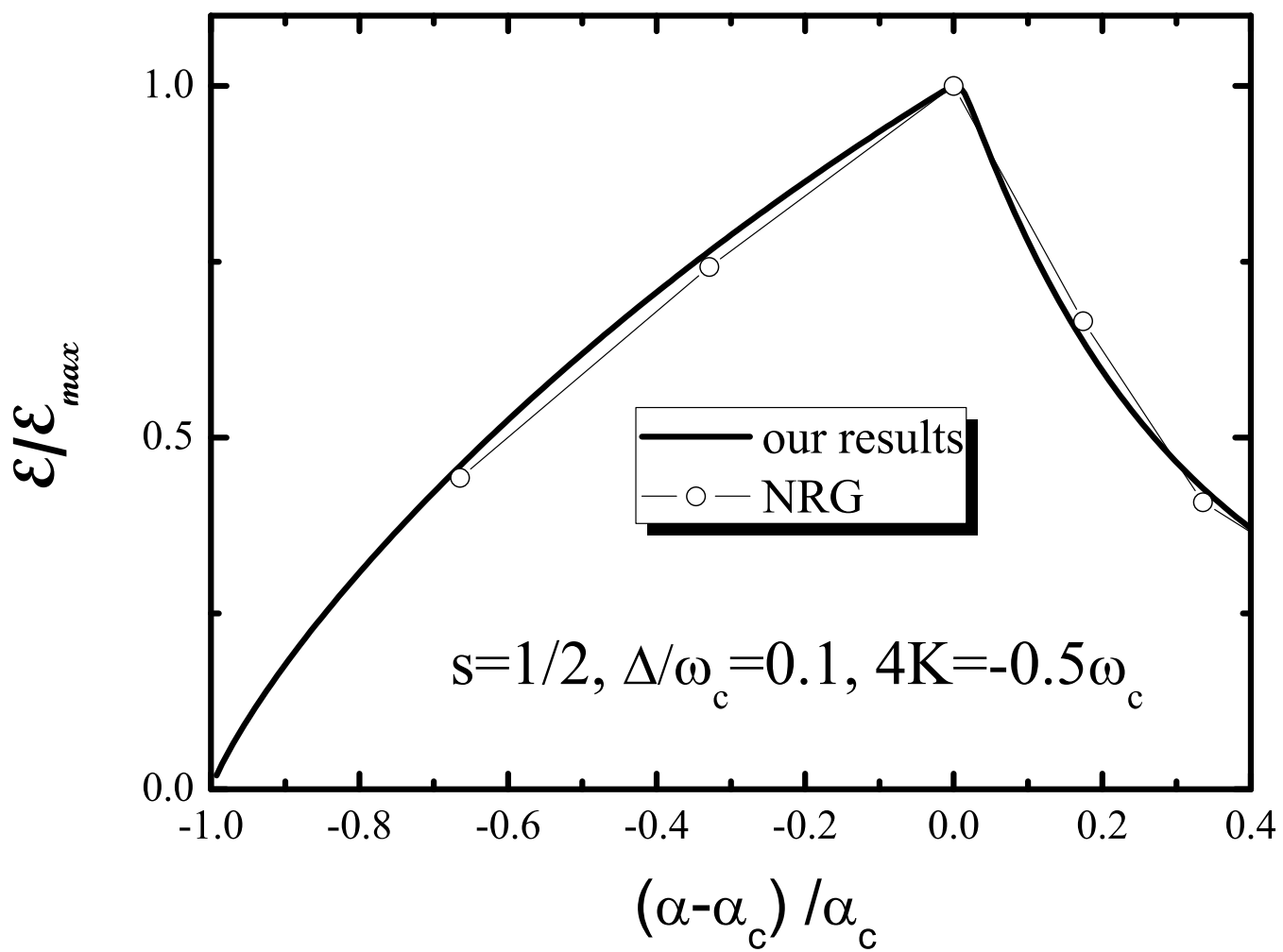
Fig.6(a)

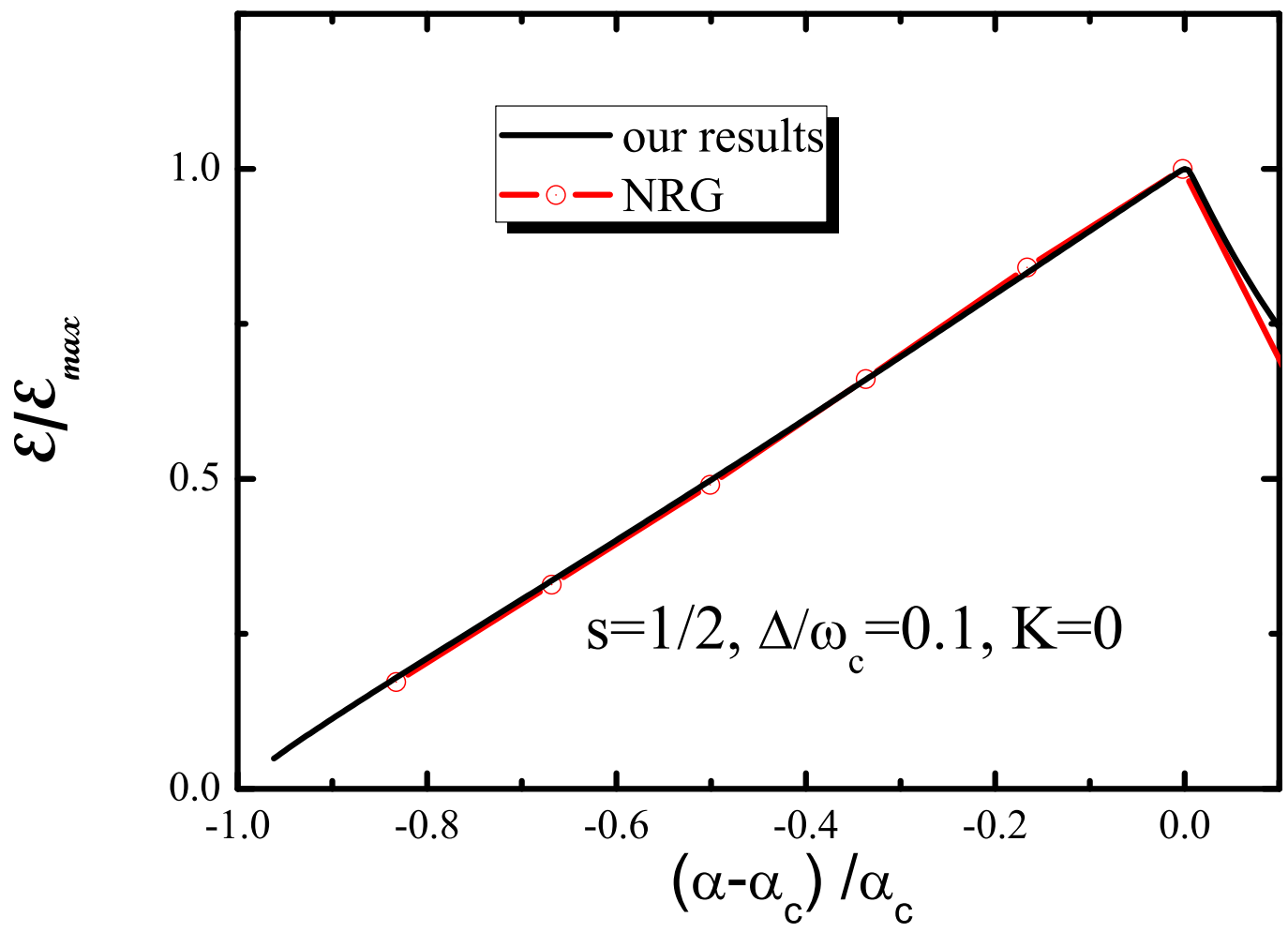


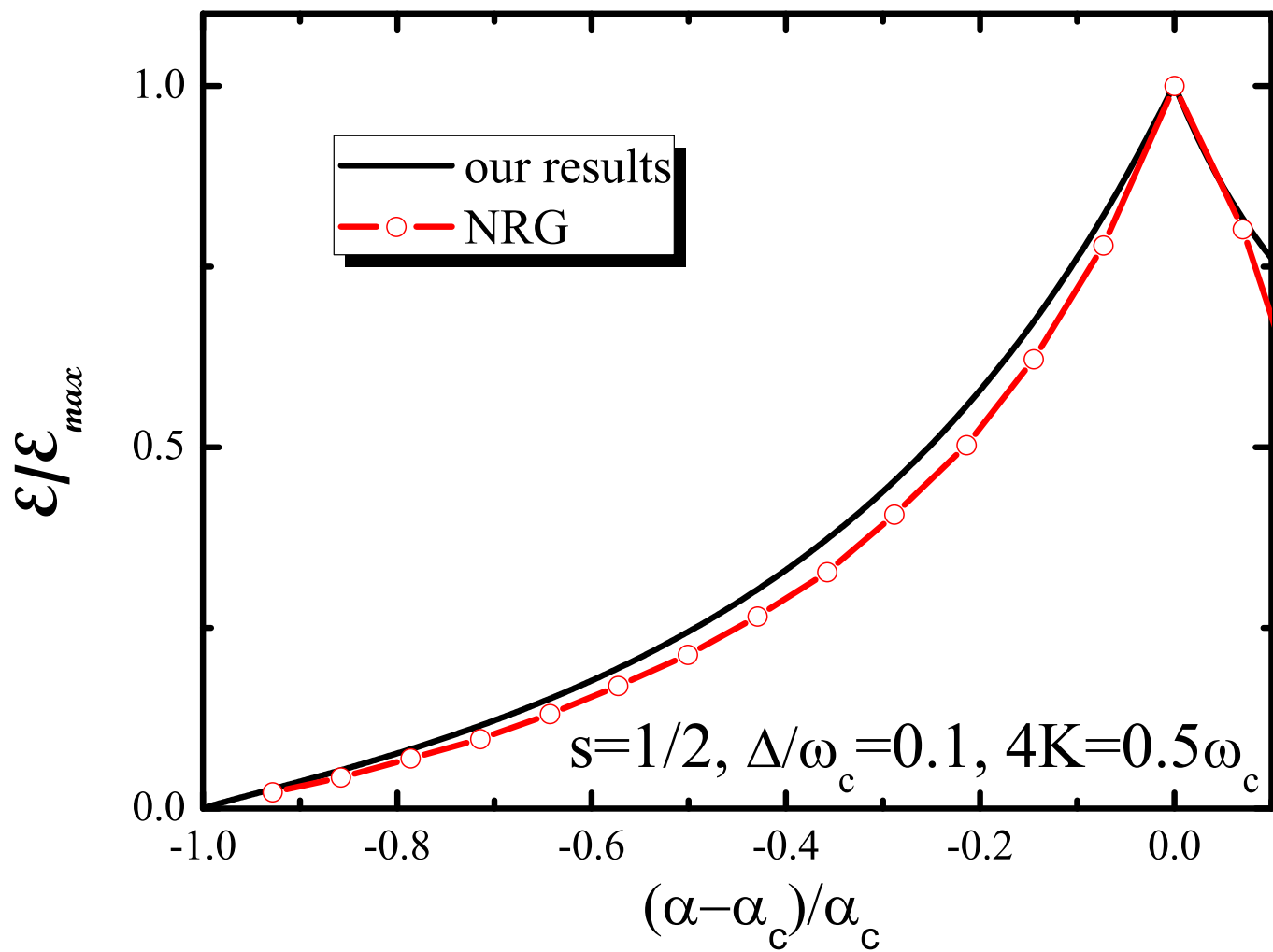


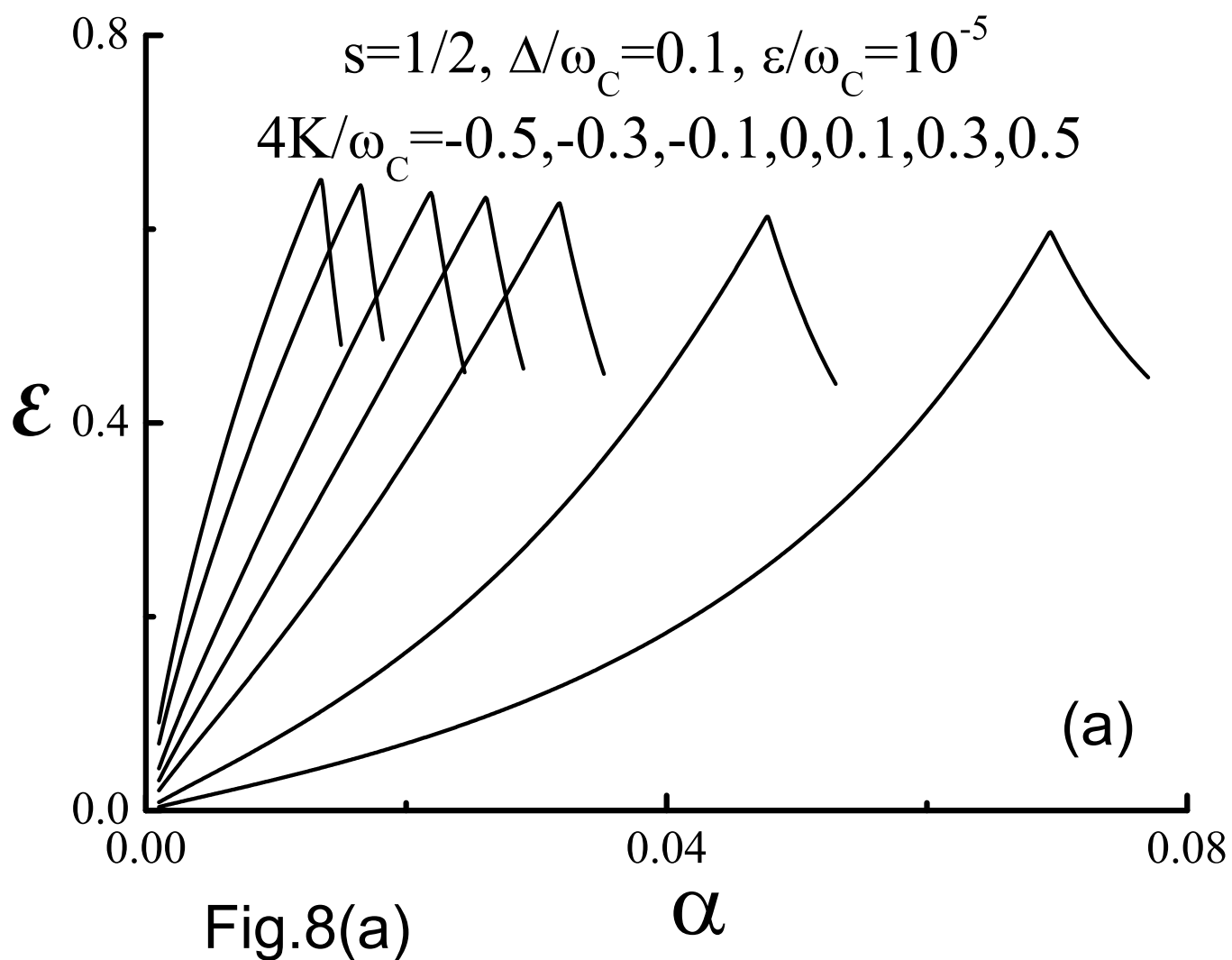












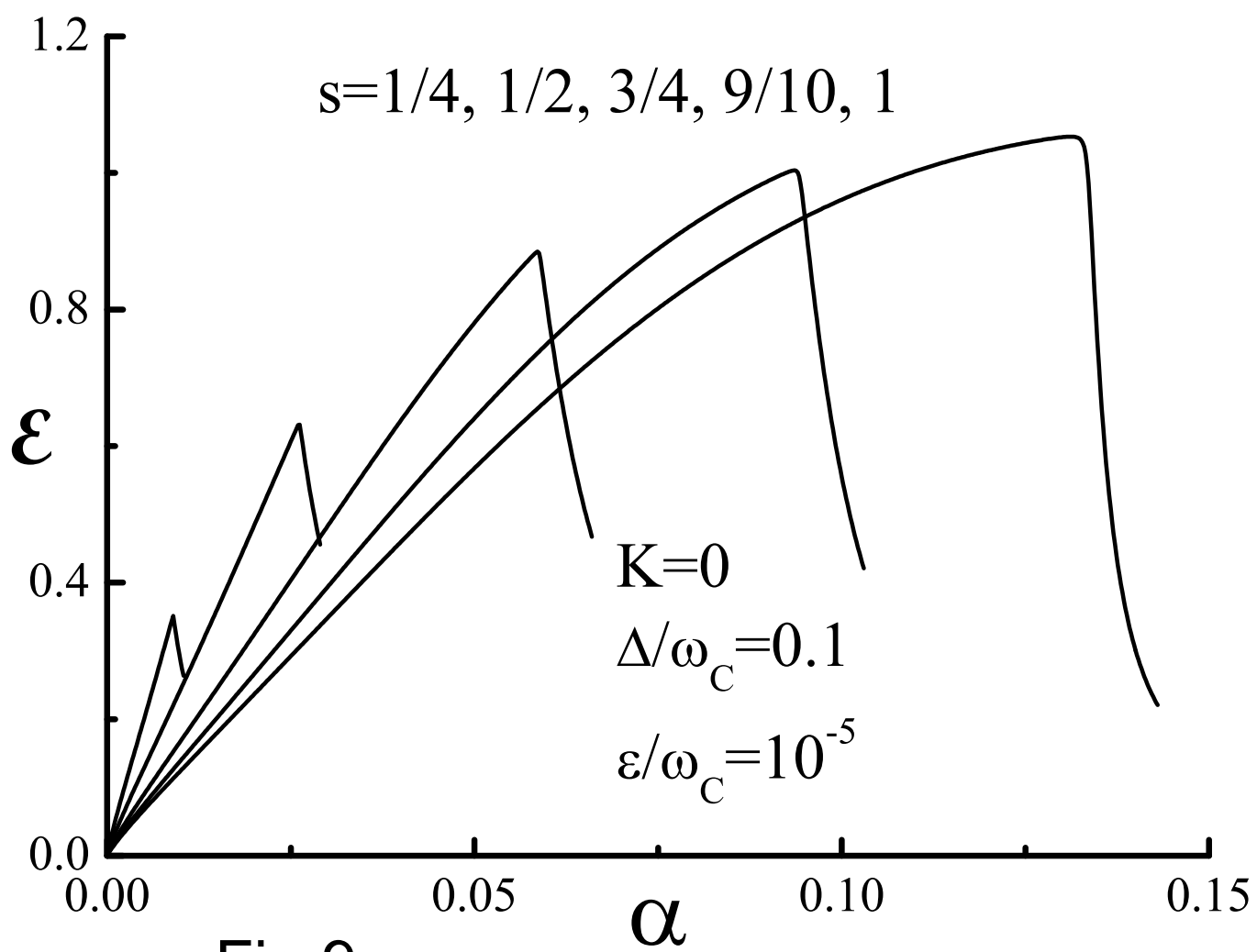
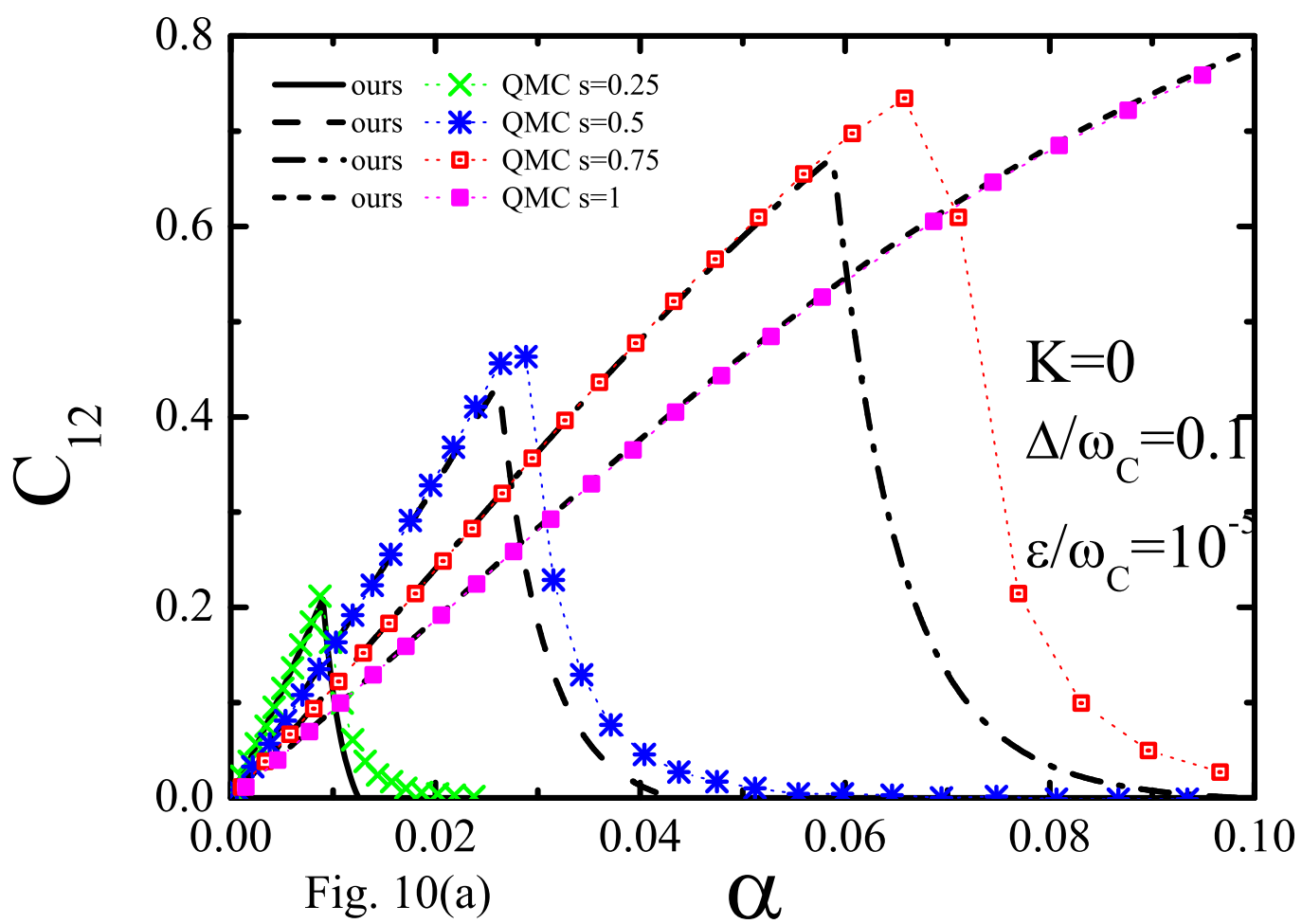


Fig.9



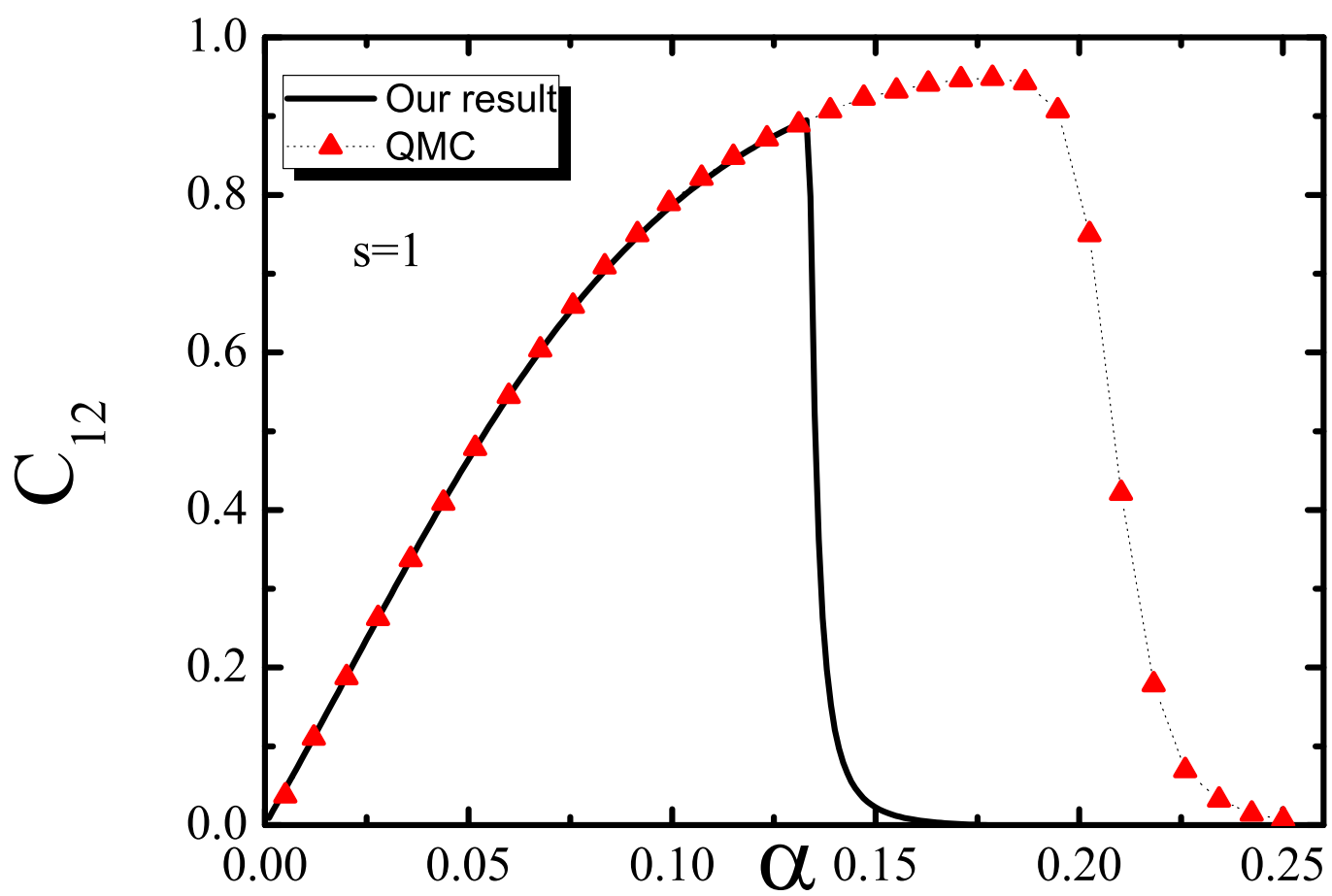


Fig. 10(b)

